1-1-1976

Crack closure and fatigue crack growth in 2219-T851 aluminum alloy.

Kurt D. Unangst

CRACK CLOSURE AND FATIGUE CRACK GROWTH IN 2219-T851 ALUMINUM ALLOY

by

Kurt D. Unangst

A Thesis

Presented to the Graduate Committee

of Lehigh University

in Candidacy for the Degree of

Master of Science

in

Applied Mechanics

Lehigh University

1976

CERTIFICATE OF APPROVAL

This thesis is accepted and approved in partial fulfillment of the requirements for the degree of Master of Science in Applied Mechanics.

Sept. 10, 1976
(date)

Professor in Charge

Chairman of Department

ACKNOWLEDGMENT

The author wishes to express his gratitude to Professor Robert P. Wei and Dr. True-Tsai Shih for their guidance during the course of this research. Their personal interest and considerable patience are deeply appreciated.

Acknowledgment is also extended to Mr. Carl D. Miller for his invaluable contribution to the experimental portion of this work.

The author gratefully acknowledges the financial support provided by a Departmental Fellowship and the Air Force Office of Scientific Research under contract AFOSR-75-2857.

TABLE OF CONTENTS

LIST OF TABLES

LIST OF FIGURES

ABSTRACT

The effects of specimen thickness, stress ratio (R) and maximum stress intensity factor (K_{max}) on crack closure (or opening) and on fatigue crack growth kinetics were studied using a 2219-T851 aluminum alloy. The crack length and the occurrence of crack closure were measured by an electrical potential method. The experimental work was carried out within the framework of linear-elastic fracture mechanics.

The experimental results show that the onset of crack closure (or opening) depends on R, K_{max}, and specimen thickness. In terms of the "effective stress intensity range ratio" (U), as defined by Elber, the results show that U tends to increase for increasing R, decrease for increasing K_{max}, and decrease with increasing specimen thickness. From these trends, it is shown that the "effective stress intensity range" (ΔK_{eff}) does not always increase with increasing stress intensity range (ΔK). The fatigue crack growth data show that the specimen thickness does not have a significant effect on crack growth in this material over the lower crack growth rate region; below about 5×10^{-6} in./cycle (1.3×10^{-5} cm/cycle). In the higher crack growth rate

region, above about 5×10^{-6} in./cycle (1.3×10^{-5} cm/cycle), the crack growth rates are higher for the thicker specimens.

The viability of the crack closure model is questioned. The experimental results show that crack closure cannot fully account for the effects of stress ratio and specimen thickness or K_{max} on fatigue crack growth. The use of ΔK_{eff} as a parameter for characterizing the mechanical driving force for fatigue crack growth is questioned.

I. INTRODUCTION

With the increased emphasis on "fail-safe" and "safe-life" design of high performance aerospace and other engineering structures, the ability to accurately predict fatigue lives and fatigue crack growth response in structural components has acquired increased importance. Linear fracture mechanics has emerged over the past fifteen years, and has developed into an important tool for fatigue and fracture analyses of structures [1-4]. In its first application, the crack tip stress intensity factor (K) or the stress intensity range (ΔK), defined by linear fracture mechanics, was proposed as the appropriate parameter for characterizing the mechanical driving force for fatigue crack growth [5]. The overall success of this concept has been well documented [3-7] and K or ΔK has been incorporated into many of the empirical relationships for describing the fatigue crack growth response; that is,

$$\Delta a/\Delta N = f(\Delta K, \text{ etc.}) \qquad (1)$$

For example, see the relationships proposed by Paris [4], Paris and Erdogan [7]. These empirical relationships, however, have been found to be inadequate for most design applications. Other modifications have been proposed in an attempt to account for the effects of stress ratio (that is, the ratio, R, between minimum and maximum stresses or stress intensity factors in a given loading cycle), and for crack

growth response near the critical stress intensity factor (K_{Ic} or K_c) and the so-called fatigue crack growth threshold (ΔK_{th}) [8-11]. Further modifications have also been proposed to account for load interaction effects [12-14] and to account for crack growth under randomized loading [4,15-19]. These modifications have been used with varying degrees of success.

More recently, the concept of crack closure, first introduced by Elber, has been used to formulate additional relationships and to provide rationale for several important aspects of fatigue crack growth [20-28]. The crack closure concept has been claimed to provide rational explanations for stress ratio effect for fatigue crack growth under constant-amplitude loading [20], and for load interaction effects on crack growth (such as crack acceleration, fatigue crack growth retardation and delayed retardation) under variable amplitude loading [20-24]. Furthermore, there is some belief that the closure concept can be applied also to account for the effects of aggressive environments on fatigue crack growth [24,25], for crack growth response near the threshold [26,27] and for crack growth under randomized loading [28]. The relevant aspects of the crack closure concept are summarized and discussed in the following paragraphs.

From experiments on a 2024-T3 aluminum alloy, Elber observed that the load versus crack-opening-displacement curves exhibited a nonlinear region at the lower load levels [20]. This behavior was interpreted in terms of crack

closure, that is, physical contact between the surfaces produced by fatigue. Elber suggested that the crack is closed at the tip over the lower portion of the loading cycle and becomes open only after the applied stress exceeded a level S_{op}, and that fatigue crack growth can occur only during that portion of the loading cycle in which the crack is fully open. Based on these suggestions, an effective stress range, ΔS_{eff}, and an effective stress range ratio, U, were defined.

$$U = \frac{\Delta S_{eff}}{\Delta S} = \frac{S_{max}-S_{op}}{S_{max}-S_{min}} \qquad (2)$$

S_{max} and S_{min} are the maximum and minimum values of the applied stress in a given loading cycle; and S_{op} is the crack opening stress. U can be defined equivalently in terms of the effective stress intensity range, ΔK_{eff}, and ΔK.

$$U = \frac{\Delta K_{eff}}{\Delta K} = \frac{K_{max}-K_{op}}{K_{max}-K_{min}} \qquad (3)$$

K_{op} is the crack opening stress intensity factor corresponding to S_{op}. Elber further suggested that it would be more appropriate to correlate fatigue crack growth rate with ΔK_{eff} and proposed the following modification to the empirical equation [20]:

$$\frac{\Delta a}{\Delta N} = A\ (\Delta K_{eff})^n = A\ (U\Delta K)^n \qquad (4)$$

where A, n are empirical constants.

Based on a limited range of data on 2024-T3 aluminum alloy, Elber suggested that the effective stress range ratio, U, is only significantly dependent on the stress ratio, R,

and independent of the stress intensity range, crack length or maximum stress intensity. For the testing conditions used, he empirically correlated U with R by Eq. 5, for R values ranging from -0.1 to 0.7 [20].

$$U = 0.5 + 0.4R \tag{5}$$

Using this empirical result, Elber showed that Eq. 4* provided a better fit to the experimental data than Paris' [4] or Forman's [8] equations.

There is little question that the crack closure concept is deceptively simple and attractive, and appears easy to apply. Even though the evidence of closure has been well documented, the concept itself and the resulting relationships have not been thoroughly and critically examined over a broad range of structural alloys and conditions. Considerable controversies exist in the literature regarding the values and interpretations of crack closure loads measured by the different experimental techniques [29-32]. On the one hand, there are methods that respond to physical contact and deformation ahead of the crack tip; such as, strain gauges [33], extensometers [20] and laser interferometry [34]. On the other hand, there are methods that only respond to the physical contact between the crack surfaces; such as the ultrasonic [24,25] and electrical potential methods [29,35], and optical interferometry [36]. The former methods measure

*Since Eq. 5 suggests that U is independent of K_{max}, then Eq. 4 (like the Paris-Erdogan relation) cannot account for crack growth behavior near ΔK_{th} and K_c.

the plasticity effects in addition to the effects of crack closure while the latter group only measures physical contact. The controversies revolve, in part, around the physical meaning of the closure measurements provided by these different methods and remain to be resolved. Much controversies exist even when the same crack closure load measurement technique is used. For example, the crack opening stress as measured by the crack opening displacement techniques is known to vary with the position of the gauges [28]. Considerable uncertainties also exist concerning the effects of other pertinent variables on the crack opening load other than stress ratio. Investigators have reported that the crack opening load depends on K_{max} [35,37], crack length [30], specimen thickness [37-39], material [35,39,40], and environment [25,29,39].

In view of these uncertainties (including the concept of effective stress intensity range), the apparent acceptance and usage of the crack closure concept at this time do not appear to be fully justified. Additional work is needed to critically examine the crack closure phenomenon and to assess its possible role in fatigue crack growth and in the development of predictive procedures for fatigue.

In this work, the influences of K_{max}, R and specimen thickness on crack closure and on fatigue crack growth, under constant-amplitude loading in an inert environment, are examined. A 2219-T851 aluminum alloy was used to complement a

previous study of crack closure and fatigue crack growth in a Ti-6Al-4V alloy [35]. Crack closure was measured by means of an electrical potential technique [35]. The experimental work was carried out within the framework of linear-elastic fracture mechanics. The viability of the crack closure model to predict fatigue crack growth is also discussed.

II. MATERIAL AND EXPERIMENTAL WORK

II.1. Material and Text Matrix

A 3-in.-thick (7.62-cm-thick) plate of 2219-T851 aluminum alloy,* (12 in. by 12 in. or 30.5 cm by 30.5 cm) was obtained from the Westinghouse Electric Corporation for use in examining the effects of specimen thickness, load ratio ($R = P_{min}/P_{max} = K_{min}/K_{max}$) and stress intensity ($K_{max}$ or ΔK) on crack closure and on fatigue crack growth. The chemical composition and room-temperature tensile properties of this plate are given in Table I.

The test matrix given in Table II was designed for examining the effects of specimen thickness, load ratio and stress intensity.

II.2. Test Specimen

Wedge-opening load (WOL) specimens, having a half-height to width ratio (H/W) of 0.486 and the same planar dimensions (Fig. 1), were selected for these studies. 0.1-, 0.2-, 0.5- and 1.0-in.-thick (0.25-, 0.51-, 1.27- and 2.54-cm-thick)

*This material is being used by Westinghouse Electric Corporation in an HFML program under Contract F33615-75-C-5064.

specimens, oriented in the longitudinal (LT) orientation [42], were machined from the 3-in.-thick (7.62-cm-thick) plate. The specimen locations within the plate were randomized in the thickness direction. An initial (or crack starter) notch, about 0.77 in. (1.96 cm) in length was introduced into each specimen by electro-discharge machining (EDM). Each specimen was precracked in fatigue through a decreasing sequence of loads that terminated at the desired load-level for the actual experiments. The precracking procedure provided a fatigue crack about 0.13 in. (0.33 cm) in length from the end of the starter notch; corresponding to a crack length of about 0.9 in. (2.29 cm). This precracking procedure ensures that the subsequent fatigue crack growth will be through material that has not been altered by the notch preparation procedure and will be unaffected by the starter notch geometry.

Stress intensity factor, K, for this WOL specimen was computed from Eq. 6 [43,44]:

$$K = \frac{P}{BW}\sqrt{a}\left[30.96 - 195.8\left(\frac{a}{W}\right) + 730.6\left(\frac{a}{W}\right)^2 - 1186.3\left(\frac{a}{W}\right)^3 + 754.6\left(\frac{a}{W}\right)^4\right] \quad (6)$$

Where P = applied load,

B = specimen thickness,

W = specimen width, and

a = crack length.

Both specimen width and crack length were measured from the line of loading, as shown in Fig. 1.

II.3. Experimental Procedures

Crack closure and fatigue crack growth (including fatigue precracking) experiments were carried out in dehumidified argon, in a closed-loop electrohydraulic testing machine operated in load control. Load control was estimated to be better than ± 1 percent. Fatigue cracks were extended by constant load-amplitude (sinusoidal wave) fatigue cycling at 5 to 10 Hz* for selected maximum loads (P_{max}) and load ratio (R); P_{max} and R being maintained constant for a given test specimen. Fatigue cycling was interrupted at a crack length of about 0.9 in (2.29 cm) and, subsequently, following each 0.1 in. (0.25 cm) of crack extension for crack closure measurements. For these crack closure measurements, the specimen was unloaded from the maximum load to the minimum load used in fatigue and reloaded to the maximum load, using the single-cycle feature of the testing machine at cyclic loading frequency of 0.01 Hz. Three such unloading-reloading sequences were made at each crack length.

An electrical potential technique was used for monitoring fatigue crack growth and for making crack closure measurements [35,45,46]. Details of this technique and of the environmental control system are described separately in the following sections. For fatigue crack growth, changes in potential (crack length) were recorded as a function of time

*Previous results suggest that there should be little or no effect of frequency on crack growth in an inert environment over this range of frequencies [45].

for subsequent conversion to growth rate ($\Delta a/\Delta N$) and K. For the crack closure experiments, autographic recordings of changes in potential versus load were made.

II.4. Crack Monitoring System

The electrical potential technique used for monitoring crack growth and crack closure is based on the change in electrical resistance of the specimen with crack length [45, 46]. A constant d.c. current was applied to the specimen, and changes in electrical potential (V) were measured between fixed points above and below the crack. A schematic diagram of the measurement system is shown in Fig. 2. During a fatigue crack growth test, V was monitored as a function of time by the potential measurement circuit and recorded on a strip chart recorder. For the crack closure experiments, changes in potential were recorded as a function of applied load on a X-Y recorder. This method has been shown to be accurate and sensitive, and to agree well with other crack measurement techniques for a number of material tested in different environments [46]. The major advantages of this technique are that it permits measurement of crack length while the crack is completely covered, thus allows complete freedom for using environmental chambers which completely cover the crack area (see next section), and that it provides a direct measure of the area of crack surfaces in physical contact during closure.

Because of the complexity of the specimen geometry, an

analytical relationship between crack length and potential was not available for the WOL specimen and an experimental calibration curve had to be established. Experimental calibration was accomplished by making simultaneous visual and electrical potential measurements of crack length on specimens fatigued in air. (See Fig. 2 for placement of potential and current leads on specimens used in this study.) The calibration results for specimens of different thickness are shown in Fig. 3 as crack length (a) versus the normalized potential values (V*).† These results show the reproducibility between specimens and confirm that the calibration curve is independent of specimen thickness. The following second degree polynomial, Eq. 7, provided the best (least-square) fit to the data, and was used as the calibration curve:

$$a = 0.792 + 3.43V^* - 1.54V^{*2} \quad (a \text{ in in.})$$
$$a = 2.01 + 8.71V^* - 3.91V^{*2} \quad (a \text{ in cm}) \qquad (7)$$

†The electrical potential method provides measurements of crack length averaged through the thickness, while the visual method gives measurements of the crack length at the specimen surface only. Crack length measurements made by these two methods would differ because of crack front curvature. The discrepancy was significant for the thicker specimen. Corrections for crack front curvature were made by measuring average crack lengths from the fatigue markings (introduced during the calibration tests by changing the load amplitude) after specimen fracture. The average crack length was computed on the basis of five measurements - one at each specimen surface, one along each of the quarter-thickness planes and one along the mid-thickness plane. The "corrected" crack lengths are used in Fig. 3 and in deriving Eq. 7.

analytical relationship between crack length and potential was not available for the WOL specimen and an experimental calibration curve had to be established. Experimental calibration was accomplished by making simultaneous visual and electrical potential measurements of crack length on specimens fatigued in air. (See Fig. 2 for placement of potential and current leads on specimens used in this study.) The calibration results for specimens of different thickness are shown in Fig. 3 as crack length (a) versus the normalized potential values (V*).† These results show the reproducibility between specimens and confirm that the calibration curve is independent of specimen thickness. The following second degree polynomial, Eq. 7, provided the best (least-square) fit to the data, and was used as the calibration curve:

$$a = 0.792 + 3.43V^* - 1.54V^{*2} \quad (a \text{ in in.})$$
$$a = 2.01 + 8.71V^* - 3.91V^{*2} \quad (a \text{ in cm}) \qquad (7)$$

†The electrical potential method provides measurements of crack length averaged through the thickness, while the visual method gives measurements of the crack length at the specimen surface only. Crack length measurements made by these two methods would differ because of crack front curvature. The discrepancy was significant for the thicker specimen. Corrections for crack front curvature were made by measuring average crack lengths from the fatigue markings (introduced during the calibration tests by changing the load amplitude) after specimen fracture. The average crack length was computed on the basis of five measurements - one at each specimen surface, one along each of the quarter-thickness planes and one along the mid-thickness plane. The "corrected" crack lengths are used in Fig. 3 and in deriving Eq. 7.

Where a = crack length

V^* = $(V-Vr)/Vr$

V_r = reference potential associated with the initial notch

V = potential at a crack length a

Accuracy of crack length measurements was estimated to be better than 1 percent. The resolution, based on a fixed working current of about 10 amperes, however, depended on specimen thickness, and was only slightly dependent on crack length. For the 1-in.-thick specimen, crack length resolution was better than 0.004 in. (0.01 cm) based on 0.1μV resolution in electrical potential. Resolution for the thinner specimens improved in inverse proportion to the specimen thickness, that is, 0.002 in., 0.0008 in. and 0.0004 in. (0.005 cm, 0.002 cm and 0.001 cm) for the 0.5, 0.2, and 0.1 in. (1.27, 0.51, and 0.25 cm) thick specimens respectively. For both the crack growth and crack closure studies, the electrical potential signal from the specimen was reduced by a preset reference d.c. signal from a six dial potentiometer. The difference signal was amplified by a high-gain d.c. amplifier and was recorded by a strip chart or X-Y recorder. Ceramic loading pins were used to isolate the specimen from the testing machine and to circumvent problems that would have been introduced by changes of contact resistance between metal pins and specimen during cyclic loading.

II.5. Environment Control System

It is known that an oxide layer could form on the fracture surfaces of specimens exposed to air. This oxide layer, having different electrical properties from a clean crack surface, can interfere with the electrical potential measurement and results in an underestimate of the extent of crack closure [35]. To circumvent this problem, the crack closure and associated crack growth studies were carried out on specimens tested in dehumidified argon [35].

Dehumidified argon was maintained around the crack by flowing argon through chambers clamped to the faces of the specimen. Dehumidification was accomplished by passing ultra-high-purity grade argon (99.999% purity) through cold traps at less than -220°F (-140°C), and through a titanium sublimation pump (TSP), before admitting the gas into the environmental chamber through a high-conductance coupling. (Thus, the TSP served a dual role - as a getter and as a pump for active residual impurities in the chamber.) The effluent from the chamber was passed through another cold trap, then through a silicone fluid back-diffusion trap before being discharged. A schematic diagram of this environment control system is shown in Fig. 4. The effectiveness of this purification system has been demonstrated by Wei and Ritter [48].

II.6. Data Reduction Procedures

II.6.a. Crack Closure. Crack closure data were determined from autographic recordings of applied load versus changes in

electrical potential (or crack length). Typical curves from a series of closure tests are shown in Fig. 5 for illustration. Unlike the case of Ti-6Al-4V alloy [35], these curves possess features that make data interpretation more difficult, and a somewhat arbitrary, but consistent, procedure had to be adopted. The rationale for the selection of this procedure and the procedure itself are described. A comparison with alternative procedures is made. A more detailed consideration of possible causes for the various features in the load versus electrical potential (crack length) curves are given in a later section (see DISCUSSIONS).

Ideally, at maximum load, the electrical potential would assume a value V(a) corresponding to the current crack length a. With unloading, it should remain at this value until the onset of crack closure, and then decreases with progressive crack closure to a lower value corresponding to the minimum load. On reloading, the potential would increase (generally on a different path) until it reaches V(a), corresponding to the onset of "full" crack opening, and then remain constant with further increase in load to the maximum load. The value of the load at which the potential reaches V(a) on reloading is defined as the crack opening load, and the corresponding point on unloading as the crack closure load.

For the 2219-T851 aluminum alloy used in this study, and for other aluminum alloys [49], the electrical potential tended to increase slightly with initial unloading before

becoming nearly constant and then decrease with further unloading (see Figs. 5 and 6). The reloading portions of the curves exhibited the same general trend, and the final indicated potential values tended to be higher than what might be expected from one cycle of fatigue crack growth. It is believed that these peculiarities were associated with changes in crack shape and with instrumental problems which became more evident in the case of these low strength, low modulus and low resistivity aluminum alloys. These peculiarities made it difficult to determine the crack opening or closure load unambiguously. To circumvent this problem and to develop a consistent and rational method for data analysis, several methods or criteria were evaluated. Two separate reference points were considered: (a) the potential (crack length) at maximum load, point A in Fig. 6, and (b) the (maximum) potential corresponding to the apparent maximum crack length (defined by a vertical tangent to the load versus potential curve), point B in Fig. 6. Only the reloading portions of the curves were considered. The various methods are illustrated schematically in Fig. 6. In Method 1, the crack opening load (P_{op}) is defined as the load at the onset of "full" crack opening, corresponding to the apparent maximum crack length (vertical tangent). Methods 2 to 5 are off-set methods and based on arbitrary choices of average crack closure lengths. Methods 2 and 3 are based on average crack closure of 0.005 and 0.010 in. (0.013 and 0.025 cm) measured from

the point of apparent maximum crack length, respectively. In Methods 4 and 5, the same average crack closure lengths are used in conjunction with the maximum load point. A comparison of K_{op} values obtained by these five methods is shown in Fig. 7. It is seen that Method 1 provided the highest estimates (although not necessarily upper bound estimates) for K_{op}, and that all five methods produced the same trend in data.

Of the two reference points considered, it is believed that the second one more closely represents a line crack. Based on this belief, Method 1 might appear to be a reasonable first choice for use in data analysis. Unfortunately, however, ambiguities are introduced because of the contravening effects of changes in crack shape and possible onset of crack closure, and because of the inherent difficulties associated with the determination of tangency points. A viable alternative appears to be Method 2, which embodies the more acceptable second reference point and provides a more easily and precisely defined (though arbitrary) intercept on the load-potential curve. Since all five methods provide the same trend, and since Method 2 yields values that fall between the other methods, it was selected for use in estimating crack opening loads in all of the experiments. It is to be recognized that the actual crack opening loads would, in all likelihood, be somewhat higher (about 10 percent) than those given by Method 2.

The indicated amount of crack closure was observed to decrease about 5 percent with each successive crack closure test at a given crack length. This apparent decrease in crack closure may be attributed to slight oxidation of the crack surfaces by the residual impurities (less than 1 ppm of H_2O and/or O_2) during the long period of unloading and reloading process (100 sec. per closure test). Since this apparent decrease in crack closure would result in successively lower crack opening loads from each of the off-set methods, only results from the first closure test at each crack length were used. The other closure tests were merely used for verification.

II.6.b. Fatigue Crack Growth Data. Fatigue crack growth rate data were obtained directly from the electrical potential (crack length) versus time (elapsed cycle) records, using the experimental calibration results, Fig. 3. Crack lengths (hence, K and ΔK) were determined from the potential values, and the corresponding growth rates were obtained by graphical differentiation of the potential-time records. Because of crack closure, corrections had to be made for some of the data at the lower R values and at high K. The cause and the correction procedures are described and discussed.

As a result of crack closure, an oscillating electrical potential signal (corresponding to the alternate opening and closing of the fatigue crack near its tip) is produced. The recorder response in the electrical potential (crack monitor-

ing) system was such that the rms (root mean square) values of this oscillating signal were recorded. At long crack lengths (that is, at high K levels) the differences between the rms values and the potential values corresponding to a fully opened crack were sufficiently large to require corrections, particularly for tests at the lower R values. (The need for this correction, however, can be eliminated by sampling only the peak values with appropriate instrumentation.) The true potential can be obtained by periodically stopping the testing machine and keeping it at the maximum value of the cyclic load. The difference between the true potential and the recorded potential, therefore, can be obtained during these interruptions. The potential values at the intermediate points, then, can be corrected by interpolation. After correcting the recorded electrical potential, the correct crack length and crack growth rate can be obtained in the usual manner. This correction procedure was used for data obtained at R of 0.05 and 0.3 at K_{max} above about 12.0 ksi$\sqrt{in}$. (13.2 MN-m$^{-3/2}$). In all other cases, the differences were negligibly small and required no correction.

III. EXPERIMENTAL RESULTS

Experimental work was directed principally at studies of crack closure and of fatigue crack growth under constant-amplitude cyclic load in a 2219-T851 aluminum alloy plate, tested in dehumidified argon at room temperature. Crack

closure and fatigue crack growth were examined as a function of K_{max}, stress ratio (R), and specimen thickness (see Test Matrix given in Table II). The crack closure results and fatigue crack growth data are described separately.

III.1. Crack Closure

Experimental results show that the onset of crack opening is a function of all of the variables studied, namely, K_{max}, stress ratio, and specimen thickness. The results are summarized and discussed in terms of the "effective stress range U", $U = (P_{max}-P_{op})/(P_{max}-P_{min})$, and the "effective stress intentisy range", $\Delta K_{eff} = K_{max}-K_{op}$, as defined by Elber [20]. It is to be emphasized that U and ΔK_{eff} are being used here solely for the sake of convenience in comparing experimental results with data reported by other investigators, and that no physical significance for these parameters is assumed or implied. These results are summarized in Figs. 8 to 15. For brevity, only those results obtained from crack opening loads determined on the basis of an average crack closure of 0.005 in. (or 0.013 cm) from the maximum apparent crack length of the loading curves are shown (see Section II.6.a.).

The effect of K_{max} on U (or crack closure) at several stress ratios (0.05, 0.3, 0.5, and 0.7) are shown in Fig. 8 and Fig. 9 for 0.5 and 0.1 in. (1.27 and 0.254 cm) thick specimens respectively. The data show that U decreases with increasing K_{max} and increases with increasing R. These trends

are consistent with previously reported results on a mill annealed Ti-6Al-4V alloy plate [35]. These results, however, are not in complete agreement with the published results on 2219-T851 aluminum alloy that suggested U to be independent of K_{max} at $0 < R < 0.32$ and to be equal to 1 (that is, no crack closure) for $R \geq 0.32$ [40]. The effect of specimen thickness on U is shown in Figs. 10 and 11 for two values of stress ratio (0.05 and 0.3 respectively). The results show that over the range of R and K_{max} studied, U tends to decrease with increasing specimen thickness. The effect of specimen thickness on crack closure tends to disappear for thicknesses larger than 0.5. This trend is not consistent with previous results of 2024-T3 aluminum alloy that showed somewhat less crack closure in the thicker specimens [38,39].

The experimental data may be presented also in terms of the effective stress intensity range (ΔK_{eff}) versus ΔK, Figs. 12 to 15. The trend lines shown were constructed from those in the U versus K_{max} plots, Figs. 8 to 11. These data simply reflect changes in U with K_{max} or ΔK, and show that ΔK_{eff} does not necessarily increase with increasing ΔK. For example, at stress ratio R = 0.05, the ΔK_{eff} increasing with ΔK at low K level and then tend to decrease with increasing ΔK for the 0.1-in. (0.254-cm)-thick specimen. On the other hand, at this stress ratio, ΔK_{eff} decreases monotonically with increasing ΔK for the 1.0-in. (2.54-cm)-thick specimen. The implications of these results are considered further in the discussion section.

III.2. Fatigue Crack Growth

Fatigue crack growth data were obtained in conjunction with the crack closure studies and are shown in Figs. 16 to 19. The achievable reproducibility of crack growth data can be readily seen from the results from duplicated tests of 0.5-in. (1.27 cm)-thick specimens at R = 0.5, Fig. 18. Data scatter was estimated to be equal to about ±20 percent. Figs. 16 and 17 show that stress ratio has a significant effect on fatigue crack growth over the range of stress ratio (R) from 0.05 to 0.7. The R effects are consistent with previous results on Ti-6Al-4V alloy [35]. They are not in agreement, however, with those of Katcher and Kaplan [40], that showed an absence of stress ratio effect for 2219-T851 aluminum alloy (tested in air) at $R \geq 0.32$.

Figs. 18 and 19 also show that specimen thickness does not have a significant effect on fatigue crack growth at the lower growth rates (that is, below about 5×10^{-6} in./cycle or 1.3×10^{-5} cm/cycle), where the condition approximating "plane strain" prevails over the range of specimen thickness (0.1 to 1.0 in.) and K levels used in this study. At the higher growth rates (that is, above about 5×10^{-6} in./cycle (1.3×10^{-5} cm/cycle)), crack growth rates tend to be higher for the thicker specimens, which is consistent with the lower values of fracture toughness for the thicker specimens [50, 51].

IV. DISCUSSIONS

The present study has provided a comprehensive set of experimental data on crack closure and on fatigue crack growth for an aluminum alloy over a range of specimen thickness, stress ratio, and K_{max} (or ΔK). The trend of these data are consistent with those obtained previously on a Ti-6Al-4V alloy as functions of stress ratio and K_{max} (or ΔK) [35]. Taken in toto, these two sets of results provide a useful basis for assessing (a) the crack closure and fatigue crack growth response to changes in K_{max}, stress ratio and specimen thickness, and (b) the crack closure (or effective stress intensity range) concept and the viability of this concept for correlating and understanding fatigue crack growth. The crack closure and fatigue crack growth results are considered separately first, and are then taken together in a critical assessment of the viability of the crack closure concept.

IV.1. Crack Closure

IV.1.a. Crack Closure Measurement. Before discussing and comparing the results of this study with other investigations, a clearer understanding of the processes that give rise to the load versus electrical potential curves or crack closure is needed.

For an idealized crack in an elastic medium, the crack surfaces are expected to be completely separated (open) under

an externally applied tensile load, and to be in complete contact (fully closed) in compression. Load vs. change in electrical potential curves for this idealized case are expected to follow the behavior indicated by Fig. 20a. In reality, crack closure is expected to proceed from the crack tip and extend gradually back towards the initial notch, as indicated in Fig. 20b. The initial deviation from V(a) can be identified with the onset of crack closure, which is associated with the crack closure stress or load. If the unloading and reloading curves follow the same path, this point can then be associated with the crack opening stress, S_{op}, defined by Elber [20].

As shown in Figs. 5 and 6, however, there was an initial increase of electrical potential upon unloading from the maximum load. This "bulge" was also observed by other investigators [29]. The most plausible cause for this bulge is believed to result from an apparent change in crack length associated with a change in the shape of the crack with loading and unloading. This process may be rationalized if one assumes the length of the crack perimeter to remain essentially constant. At the maximum load, the crack is approximately parabolic (or ellipical for center cracked specimens) in shape. With unloading, the parabola (or ellipse) is collapsed. The resulting change in shape produces an apparent increase in crack length, thus causing the resistance and the electrical potential to increase. An

order of magnitude estimate of this effect showed that this process could account for the observed changes in potential and provided justification for the use of the indicated apparent maximum crack lengths as reference points for data analysis (see section II.6.a).

The records (see Figs. 5 and 6) also showed that during the reloading process, the electrical potential remained essentially constant initially and was less than that at the corresponding load during unloading. This difference can be attributed to the refracturing of regions of the crack surfaces that had become "cold welded" during unloading, and lends further support for the occurrence of crack closure. As the reloading process is continued, the potential eventually crossed over the unloading curve and attained a value at the maximum load that was higher than the potential before unloading, Fig. 5. The difference in potential indicated an apparent crack growth that was much larger than the growth associated with one loading cycle. This difference is believed to be artifactual (probably related to recorder "backlash") and would introduce only minor errors into the opening load measurements.

It is to be emphasized that the electrical potential method provides closure (or opening) load measurements directly related to physical contact of the crack surfaces. Because of the aforementioned uncertainties, the crack opening loads, and the associated values of U and ΔK_{eff} do not

represent the "true" values for this 2219-T851 aluminum alloy. They do, however, represent best estimates of these parameters and portray the correct trends in behavior. Comparisons with other investigations are to be considered in light of these comments.

IV.1.b. Phenomenology of Crack Closure. There is now agreement that crack closure does occur during fatigue, and that the crack opening load would depend on the inter-relationship between the crack opening displacement produced by the externally applied load (for the elastic-plastic case) and the effective thickness of the layer of residual tensile deformation* left in the wake of the fatigue crack tip [20,35]. This inter-relationship would, in turn, determine the variation of U (the effective stress intensity range ratio) with K_{max} and with specimen thickness. In an earlier study on crack closure in a Ti-6Al-4V alloy, Shih and Wei [35] suggested that the surface shear lip associated with fatigue crack growth played a dominant role in crack closure. The shear lip contributions should be incorporated into the considerations of the present results on 2219-T851 aluminum alloy.

*Residual tensile deformation is viewed here, in a broad sense, to include the contributions from the crack-tip plastic zone (including the surface shear lip) and the localized deformation associated with fatigue fracture on a microstructural scale.

At the very low K_{max} levels, the increment of crack growth per cycle is very small (of the order 10^{-5} times the crack-tip plastic zone size) and represents an average of crack advance at localized positions along the crack front. The fracture process tends to be on an microstructural scale and involves very localized deformation [52]. As such, the effective thickness of the residual tensile deformation layer (including the shear lip contribution) is expected to be smaller than the crack opening displacement at K_{min}. Consequently, U is expected to be equal to 1.0 in this region (see Fig. 21). (Alternatively, one can consider that the crack behaves essentially as an elastic crack and arrive at the same conclusion that U would be equal to 1.0 in the very low K_{max} range.) As K_{max} is increased, the crack growth increment becomes a larger fraction of the plastic zone size (of the order of 10^{-3} times) and represents a more uniform increment of advance along the entire crack front. The size of the accompanying surface shear lip and the effective thickness of the residual tensile deformation layer are also expected to increase. The increase must be such as to cause crack closure and the subsequent crack opening to occur at a K level above K_{min} and to cause a decrease in U with increasing K_{max}. With further increases in K_{max}, the size of the surface shear lip is expected to become stabilized, whereby U is expected to reach a minimum value and than begin to increase (Fig. 21).

In the limit, U is expected to tend toward 1.0 as K_{max} becomes sufficiently large to cause large scale yielding ahead of the crack tip. The observed variation of U with K_{max} (Figs. 8 and 11) lends support to the foregoing simple physical view of the crack closure phenomenon.

Because K_{min} increases with R and because the effective thickness of the residual tensile deformation layer is not expected to depend strongly on R, the value of K_{max} at which U departs from 1.0 is expected to increase with K_{max}. Similarly, U is expected to increase with R at a given K_{max}. These trends are consistent with the experimental observations (Figs. 8 and 9).

If the surface shear lip plays a significant role in crack closure, one could expect (at a given K_{max}) U to decrease with specimen thickness and then remain essentially constant with further increases in specimen thickness. This expectation is based on the facts that (a) the shear lip size tends to remain constant at a given K_{max}, and (b) the crack opening displacement tends to decrease with increasing specimen thickness as the crack-tip constraint changes from one of essentially plane-stress to that approximating plane-strain. Such a change in U with specimen thickness is consistent with the experimental data (see Figs. 10 and 11).

It is seen that U is a complex function of K_{max} and of specimen thickness. The observed variations in U are consist-

ent with a simplified physical view of the closure phenomenon that involve considerations of the role of surface shear lip associated with crack growth. As such, crack closure must be viewed as a 3-dimensional phenomenon [35] and must be treated as such in any rational analysis.

IV.1.c. Comparisons with Other Investigations. The foregoing discussions (Sections IV.1.a and IV.1.b) have shown that the observed variations in U (the effective stress intensity range ratio) with K_{max}, R and with specimen thickness for the 2219-T851 aluminum alloy represent the best estimates of the values of U and of the data trend, and are consistent with physical reasoning. These results may now be used for comparison with the results and for assessment of the conclusions from other investigations.

Comparison of the results from this investigation with that of a previous study on Ti-6Al-4V alloy [35] indicates that the overall trends of the data are similar, although the specific dependence on stress ratio differs. The similarity between these two sets of results suggests that the general trend for the variation of U with K_{max} and R depicted by the data would hold for all materials. Differences in detail can be expected as a result of differences in material properties. These results confirm that the variation of U with K_{max} is complex and is a function of stress ratio and specimen thickness (or state of stress). U can decrease, remain sensibly

constant or increase with increasing K_{max} (at a given stress ratio and specimen thickness) depending on the range of K_{max}. Direct comparisons with other investigations, therefore, must be made with care and within the same range of K_{max}. Furthermore, these data show (see Figs. 8 to 11) that the value of U and any empirical representation of U as a function of R (such as that given by Elber [20]) would depend on the level of K_{max}, and that broad generalizations based on limited data would not be warranted.

Direct comparison between the present results and limited results on crack closure on another 2219-T851 aluminum alloy, obtained by Katcher and Kaplan [40], can be made. The results of Katcher and Kaplan covered a range of K_{max} values from about 7 to 17 ksi$\sqrt{in}$. (or 7.7 to 18.7 MN-$m^{-3/2}$) at R of 0.08, 0.3, 0.5, and 0.7. For those cases where the maximum load was maintained fixed, the U values reported by these authors are in reasonable agreement with those of this investigation*. Unfortunately, however, because of the very limited amount of closure data and of an unwarranted assumption that U is independent of K_{max}, the authors erroneously concluded the crack closure is limited to R values below about 0.32 and that U can be represented by an empirical relation, $U = 0.68 + 0.91R$, for all K_{max} levels.

*U values for R of 0.5 and 0.7 are taken to be equal to 1.0 in accordance with the definition for U.

One can infer from the present results that Elber's closure data on 2024-T3 aluminum alloy [20] must have been obtained over a region of K_{max} in which U is sensibly independent of K_{max}. The empirical relation $U = 0.5 + 0.4R$ can be valid, at best, over the K_{max} range used in his investigation, and its use must be restricted to that particular alloy and for the thickness of material used in his closure experiments. Elber's conclusion that U is independent of K_{max} [20], which was based on limited data, can no longer be accepted as being valid over a broad range of K_{max} values.

IV.2. Fatigue Crack Growth

Data on fatigue crack growth kinetics developed during this investigation show a definite effect of stress ratio on fatigue crack growth, in terms of K_{max} or ΔK (see Figs. 16 to 19). The observed dependence of crack growth rates on R is consistent with that reported previously on a Ti-6Al-4V alloy [11]. No apparent effect of specimen thickness was observed at the lower K_{max} levels, where crack growth was under essentially plane strain conditions. At the higher K_{max} levels, some thickness effect was observed; this effect is related to changes in fracture toughness with specimen thickness.

Comparison of the data from this investigation with those reported by Katcher and Kaplan [40] on another 2219-T851 aluminum alloy shows that the rates reported by Katcher and Kaplan are consistently higher at a given K_{max} and R. This

difference can be attributed to the effect of atmospheric moisture on fatigue crack growth [54], since the experiments reported by Katcher and Kaplan were carried out in low humidity air while the present experiments were performed in dehumidified argon. There is substantial disagreement, however, between the present results and the conclusion of Katcher and Kaplan with respect to the effect of stress ratio on fatigue crack growth. Based on their data, Katcher and Kaplan concluded that there was no effect of R on fatigue crack growth above R of about 0.32 [40]. Careful examination of their experimental data shows, however, that there were only four data points at (nearly equal) low K values for R = 0.7, and that the data scatter was such that the effect of R could not have been discerned from the logarithmic representation of experimental data. It appears that their conclusion had been influenced by their interpretation of the very limited amount of crack closure measurements (see Section IV.1.c), and is not fully justified. Similarly, their conclusion with respect to the crack closure model [40] in accounting for stress ratio effect on fatigue crack growth must be questioned.

IV.3. Assessment of the Crack Closure Concept

A review of the published literature shows that the crack closure concept, as it applies to fatigue crack growth, has

acquired a substantial following [21-28, 38, 55-58] since its introduction by Elber in 1970 [20]. Critical examinations of many of these publications, however, show that in spite of the apparent popularity, the underlying support for this concept is relatively weak. Much of the early interest and purported support are based on the "success" of the crack closure concept (or the use of the effective stress intensity range, ΔK_{eff}) to account for the influence of stress ratio on constant-load-amplitude fatigue crack growth. It is now quite clear that the "success" was based on a rather tenuous assumption regarding the independence of U (the effective stress intensity range ratio) on K_{max}, and on a less than critical assessment of the data (see Sections IV.1.c and IV.2). In many cases, correlations between crack growth rates with ΔK_{eff} were claimed on the basis of ad hoc assumptions of the validity of the closure concept and of the form of the relation for U (U = A + BR)*, without any independent crack closure measurements [21, 22, 55, 56]. As such, these reported results do not constitute valid support for the closure concept. In addition, there has been no direct verification of the closure concept. The only "direct"

*One can always obtain a relation of the form U = A + BR (where A and B are constants) to correlate fatigue crack growth data as a function of R over a limited range of growth rates. Such a correlation neither depends on the existence of crack closure nor supports the validity of the closure concept.

experiment that has been advanced in support of this concept [22] (in which it was claimed that the removal of the residual tensile deformation layer in the wake of the crack tip increased the rate of crack growth) is in itself suspect. In this experiment, major portions of the fatigue crack surfaces were removed by mechanical means (saw cut). The most important portion (near the crack tip) for crack closure, however, was not removed. Taken in conjunction with the fact that the mechanical process of surface removal can disturb the remaining crack surfaces and material near the crack tip, the claim of this experiment becomes highly questionable.

The crack closure results and the companion fatigue crack growth data from this investigation raise additional questions with regard to the crack closure concept. Figs. 12 to 15 show that ΔK_{eff} can in fact decrease with increasing ΔK in certain cases, which in turn is no longer compatible with the observed increases in fatigue crack growth rates. These results show further that ΔK_{eff} can depend on specimen thickness. This thickness dependence for ΔK_{eff} is inconsistent with the essential independence of crack growth rates on thickness over the lower range of K_{max} and with the higher growth rate exhibited by the thicker specimens at higher K_{max} levels (see Figs. 18 and 19). Taken in toto, these data tend to suggest that ΔK_{eff}, as it is currently defined, does not represent a proper characteri-

zation of the mechanical driving force for fatigue crack growth.

The absence of substantive support and the failure of the closure concept to account for various aspects of constant-load-amplitude fatigue crack growth raise serious questions regarding the validity of the crack closure concept; at least in the simplified form proposed by Elber and used by Elber and by others. The extension of this concept to the more complex problems of fatigue crack growth and life prediction under variable amplitude loading, therefore, does not appear to be warranted.

V. CONCLUSIONS

On the basis of experimental results obtained during this investigation on 2219-T851 aluminum alloy, the following conclusions can be made:

(1) Crack closure does occur during fatigue. For the 2219-T851 aluminum alloy, closure was observed at stress ratios between 0.05 and 0.7, and for specimen thicknesses ranging from 0.1 to 1.0 in. (0.254 to 2.54 cm).

(2) The stress intensity factor at the onset of full crack opening (or the onset of closure) and the associated stress intensity range ratio (U) depend on the maximum stress intensity factor (K_{max}), stress ratio (R), and specimen thickness (or state of stress). U can decrease, remain

sensibly constant or increase with increasing K_{max}, and tends to increase with increasing R and decrease with increasing specimen thickness (or with increasing tendency towards plane strain). The observed thickness dependence provides further support for the fact that crack closure is a 3-dimensional phenomenon and is not likely to be amenable to 2-dimensional treatment.

(3) Data on fatigue crack growth kinetics indicate a systematic effect of stress ratio and a minor effect of specimen thickness. At the lower growth rate region, specimen thickness does not have a significant effect on fatigue crack growth in this alloy. In the higher growth rate region, higher growth rates were observed for the thicker specimens.

(4) No sensible correlation could be made between the fatigue crack growth kinetics and ΔK_{eff} obtained from the crack closure studies. Hence, the effective stress intensity concept, based on crack closure, it not able to account for the various aspects of fatigue crack growth under constant amplitude loading. Its extension, in its present form, to the more complex problems of fatigue crack growth and fatigue life prediction under varialbe amplitude loading does not appear to be warranted.

Table I

Chemical Composition and Tensile Properties of 3-in.-thick (7.62-cm-thick) 2219-T851 Aluminum Alloy Plate[1]

Chemical Composition (Weight Percent)

Cu	Zn	Mg	Si	Mn	Ti	Cr	Fe	Al
6.28	0.025	0.003	0.088	0.25	0.051	<0.0001	0.25	Balance

Tensile Properties[2]

Orientation	Yield Strength ksi(MPa)	Tensile Strength ksi(MPa)	Elongation in 2 in. (5.08 cm) Percent	Reduction of Area Percent
Longitudinal	52 (358)	66 (455)	8.5	19
Transverse	51 (351)	66 (455)	8.2	19

(1) Data from Westinghouse Electric Corporation [41].

(2) Averages of 6 tests from 2 locations.

Table II

Test Matrix for Studying the Influences of K_{max}, Stress Ratio and Specimen Thickness on Crack Closure

Specimen Thickness** (in.)	Stress Ratio, R				Range of K_{max}* (ksi$\sqrt{in}$.)
	0.05	0.03	0.5	0.7	
0.1	X	X	X	X	8-30
0.2	X	X			8-30
0.5	X	X	X	X	8-30
1.0	X	X			8-30

*Approximate range of K_{max}; actual values depend on the stress ratio. 1 ksi$\sqrt{in}$ = 1.099 MN-m$^{-3/2}$.

**1 in. = 2.54 cm.

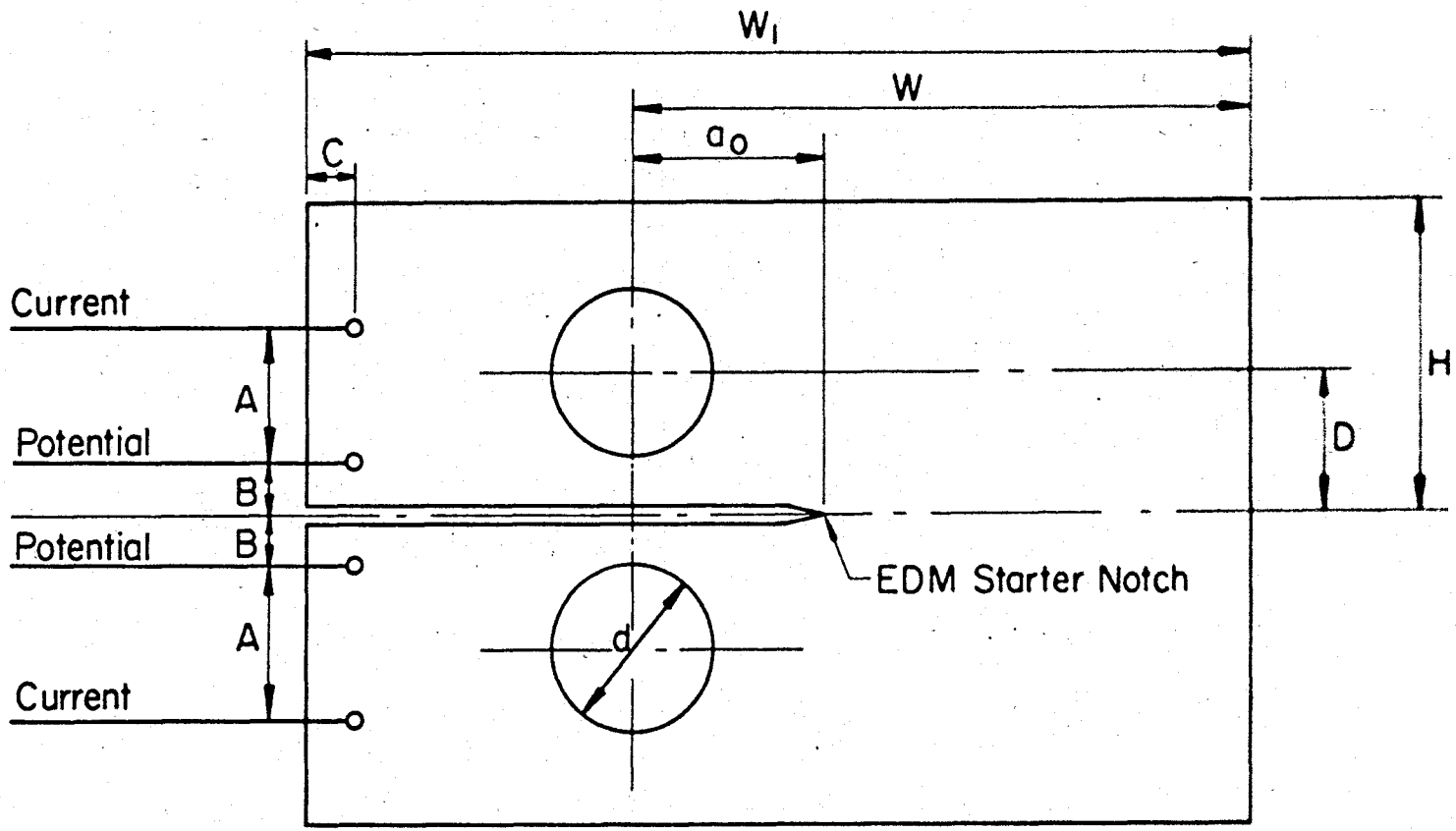

	A	B	C	W_1	W	a_0	D	H	d
ENGLISH (in.)	0.55	0.20	0.20	3.9	2.550	0.767	0.55	1240	0.625
METRIC (cm)	1.4	0.5	0.5	9.9	6.48	1.95	1.4	3.15	1.59

Figure 1: Wedge-Opening-Load (WOL) specimen and electrical potential lead placement.

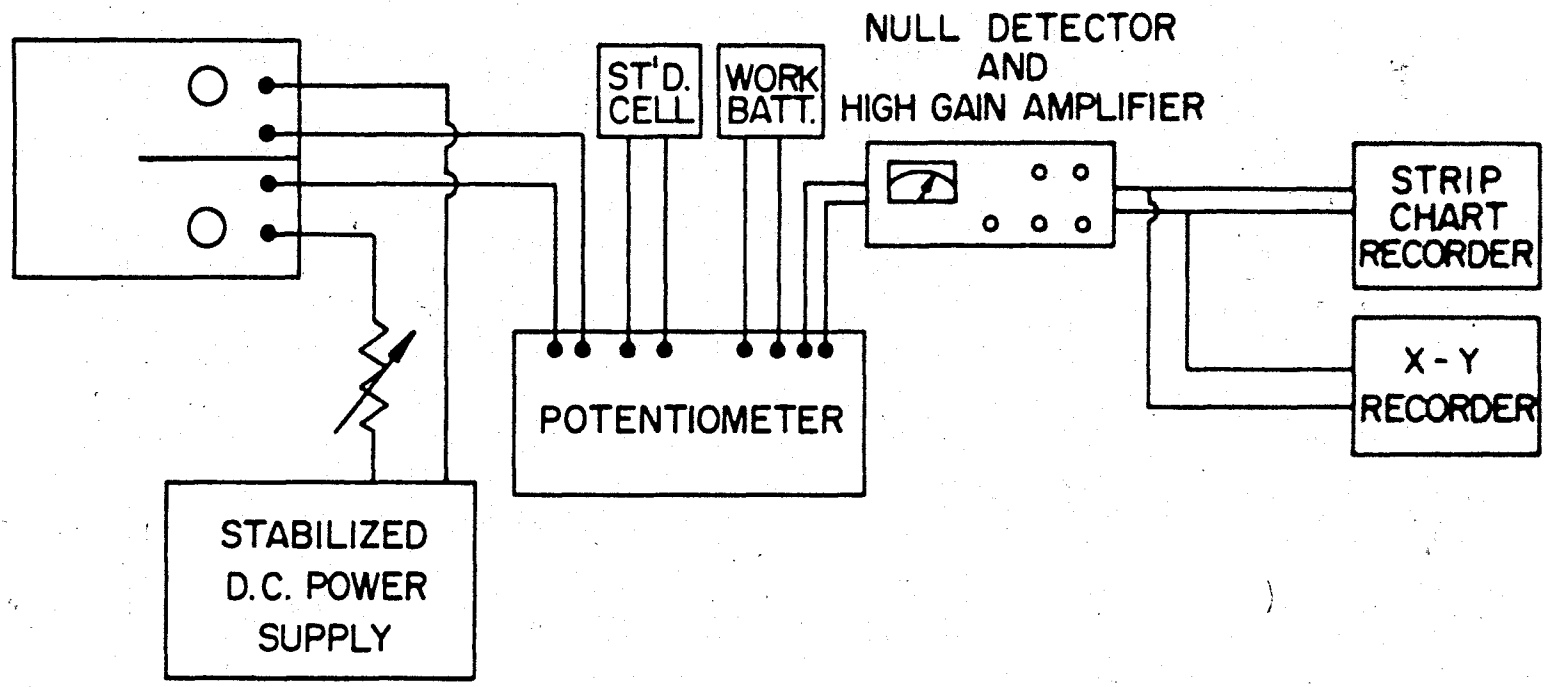

Figure 2: Schematic diagram of electrical potential system for crack length measurement.

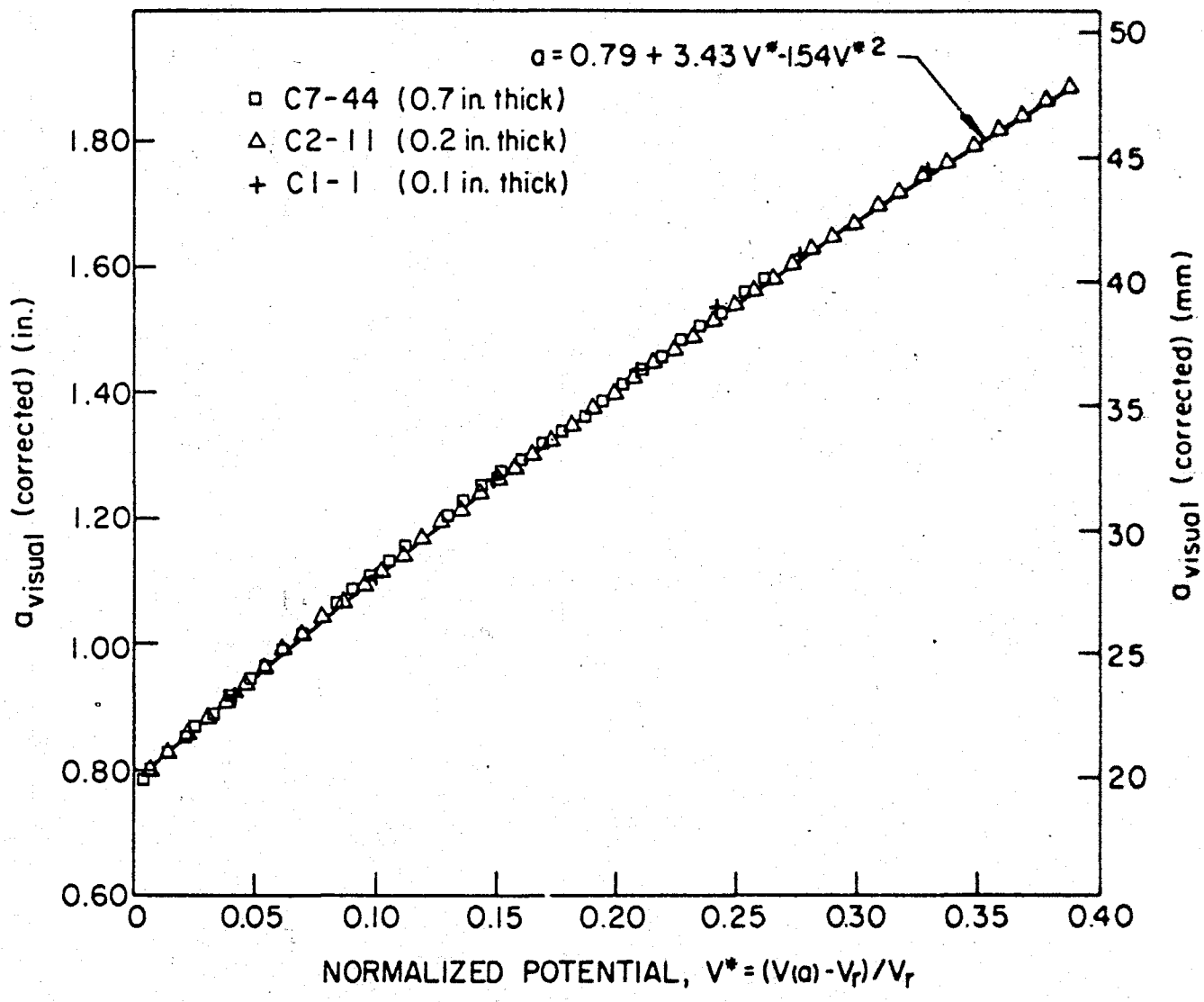

Figure 3: Electrical potential versus crack length calibration curve.

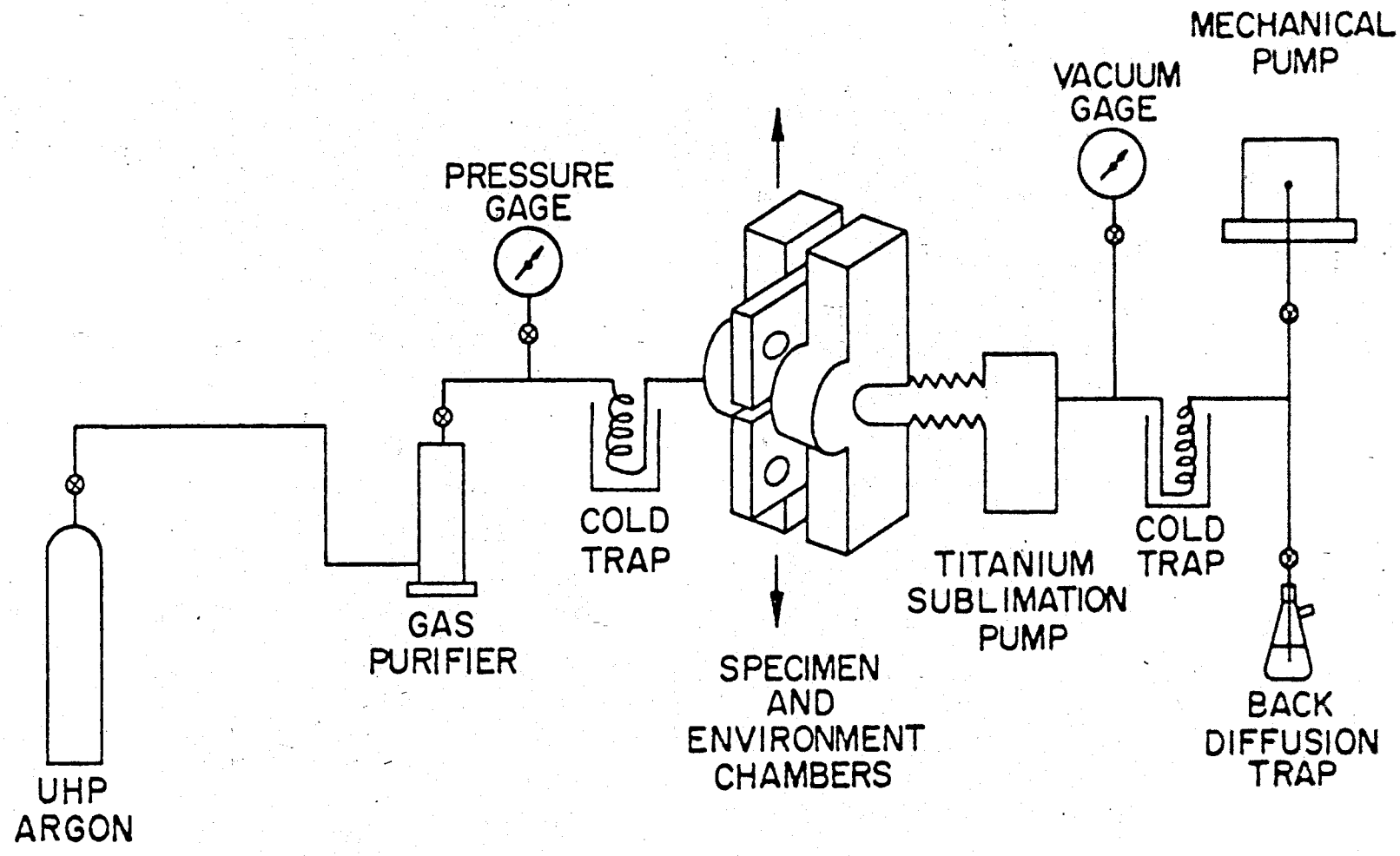

Figure 4: Schematic diagram of environment control system.

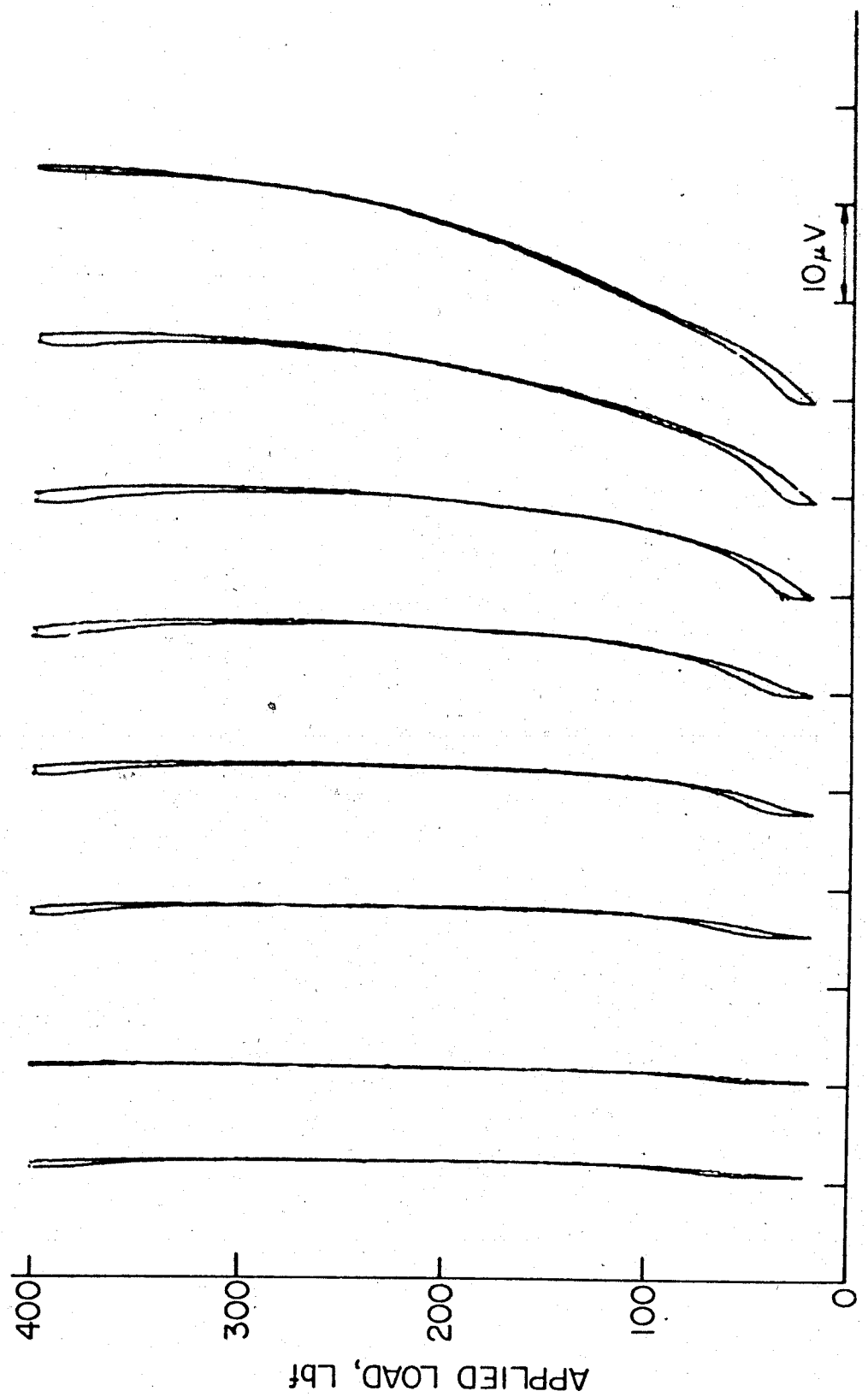

Figure 5: Typical load versus electrical potential (crack length) records from a closure test series.

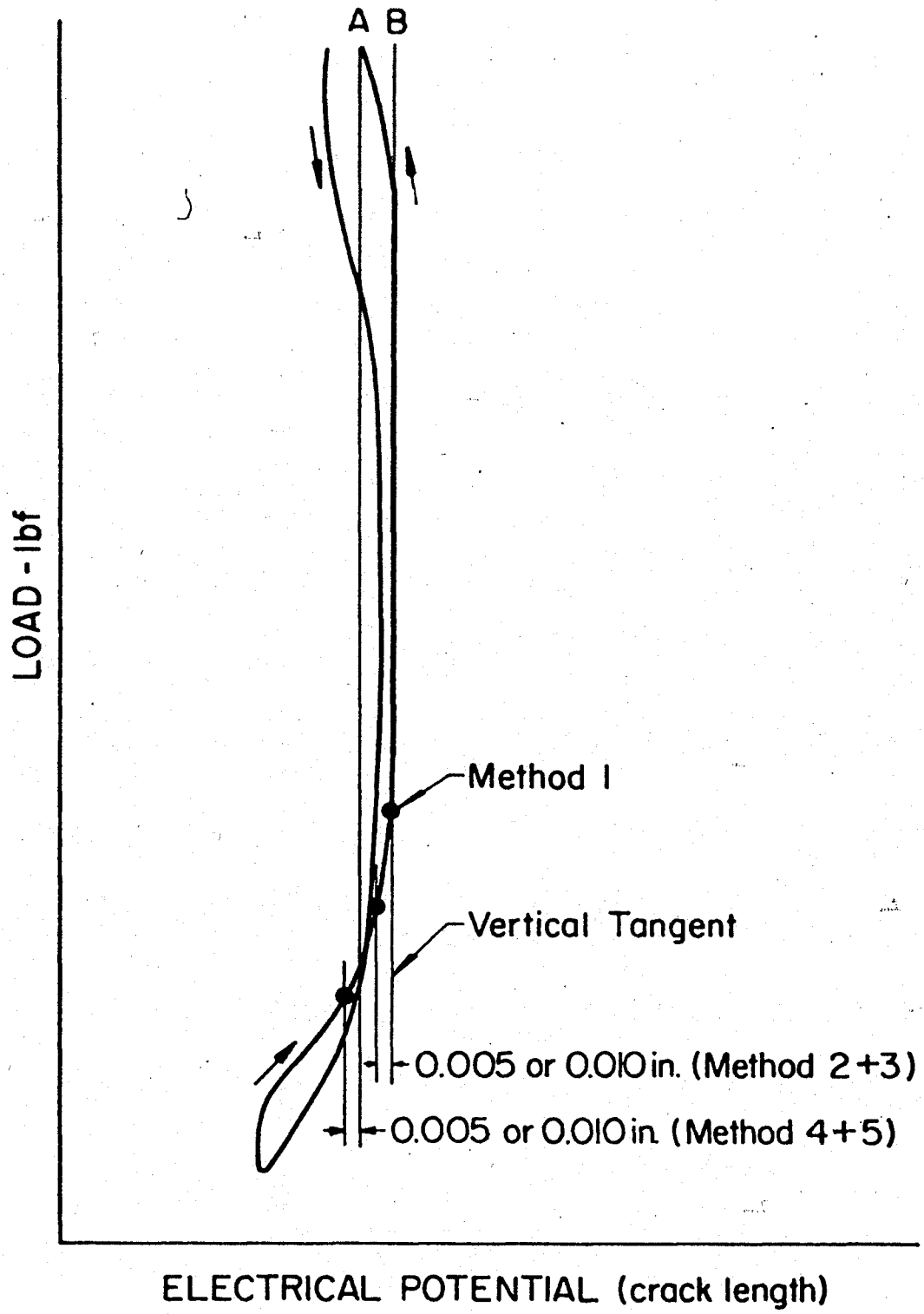

Figure 6: Illustration of different methods used for estimating crack opening load (P_{op}).

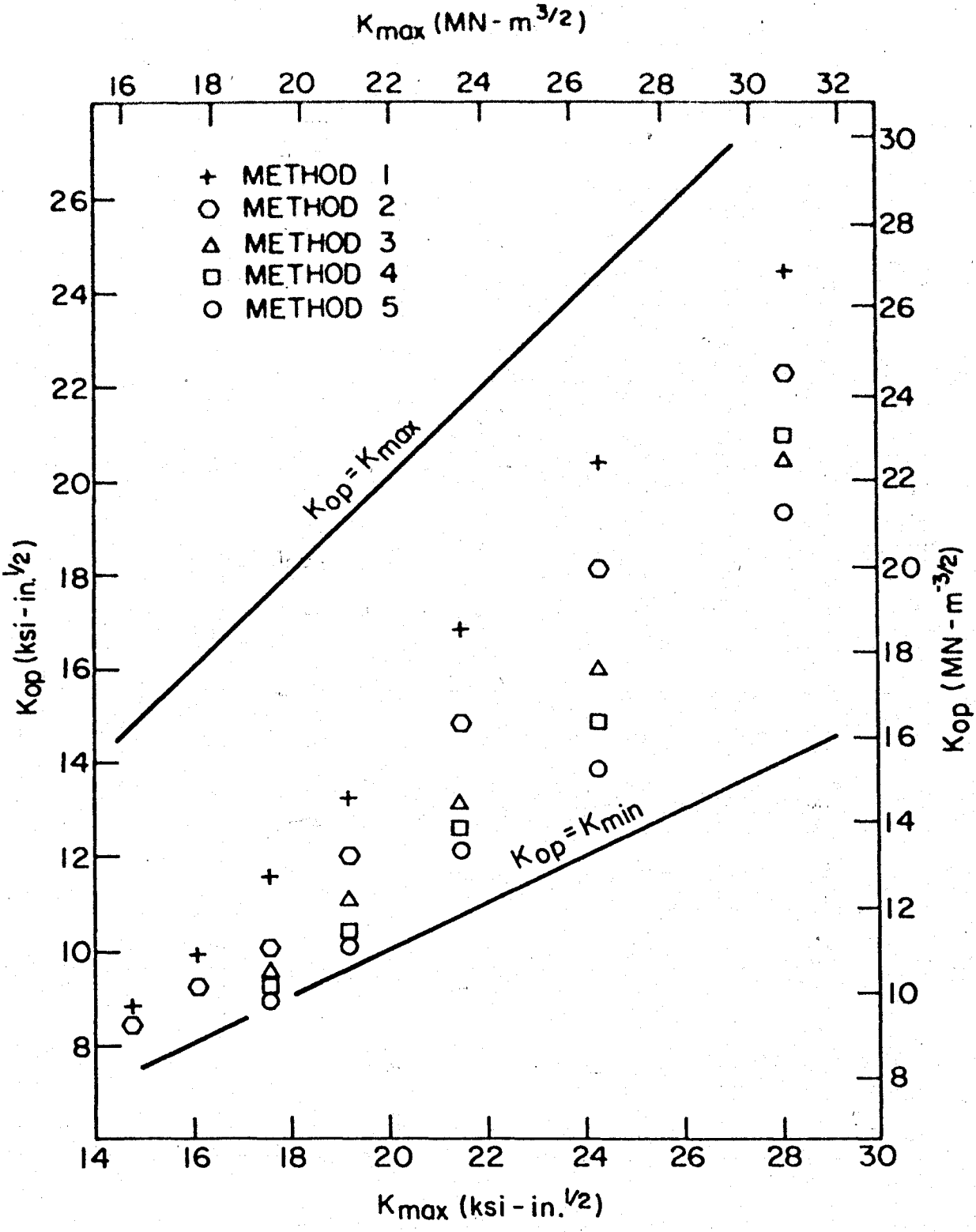

Figure 7: Illustrations of the variation of K_{op} with K_{max} obtained by the different estimation methods in Figure 6.

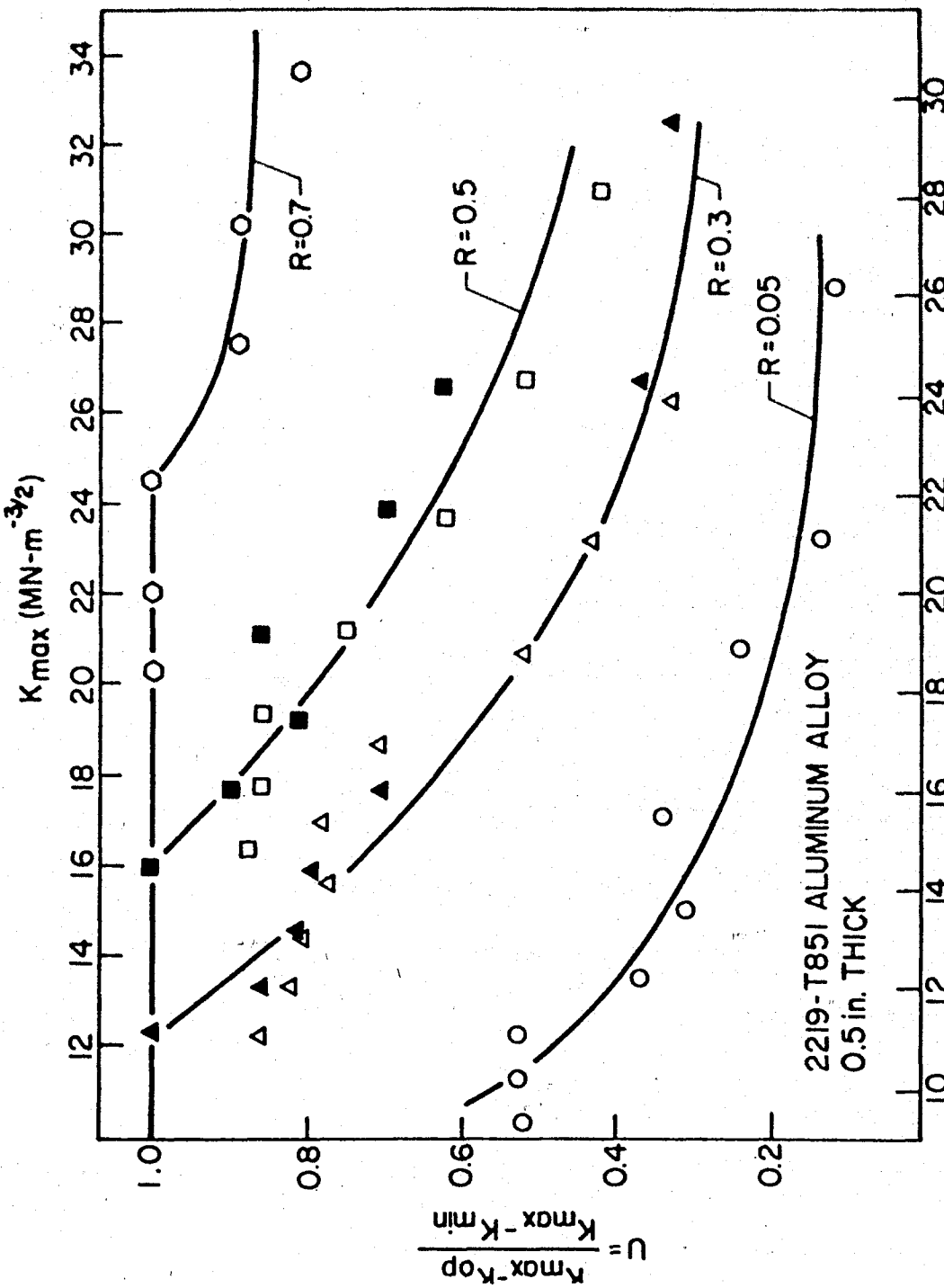

Figure 8; Relationship between U and K_{max} at different stress ratios for 0.5-in.(1.27 cm) thick specimens.

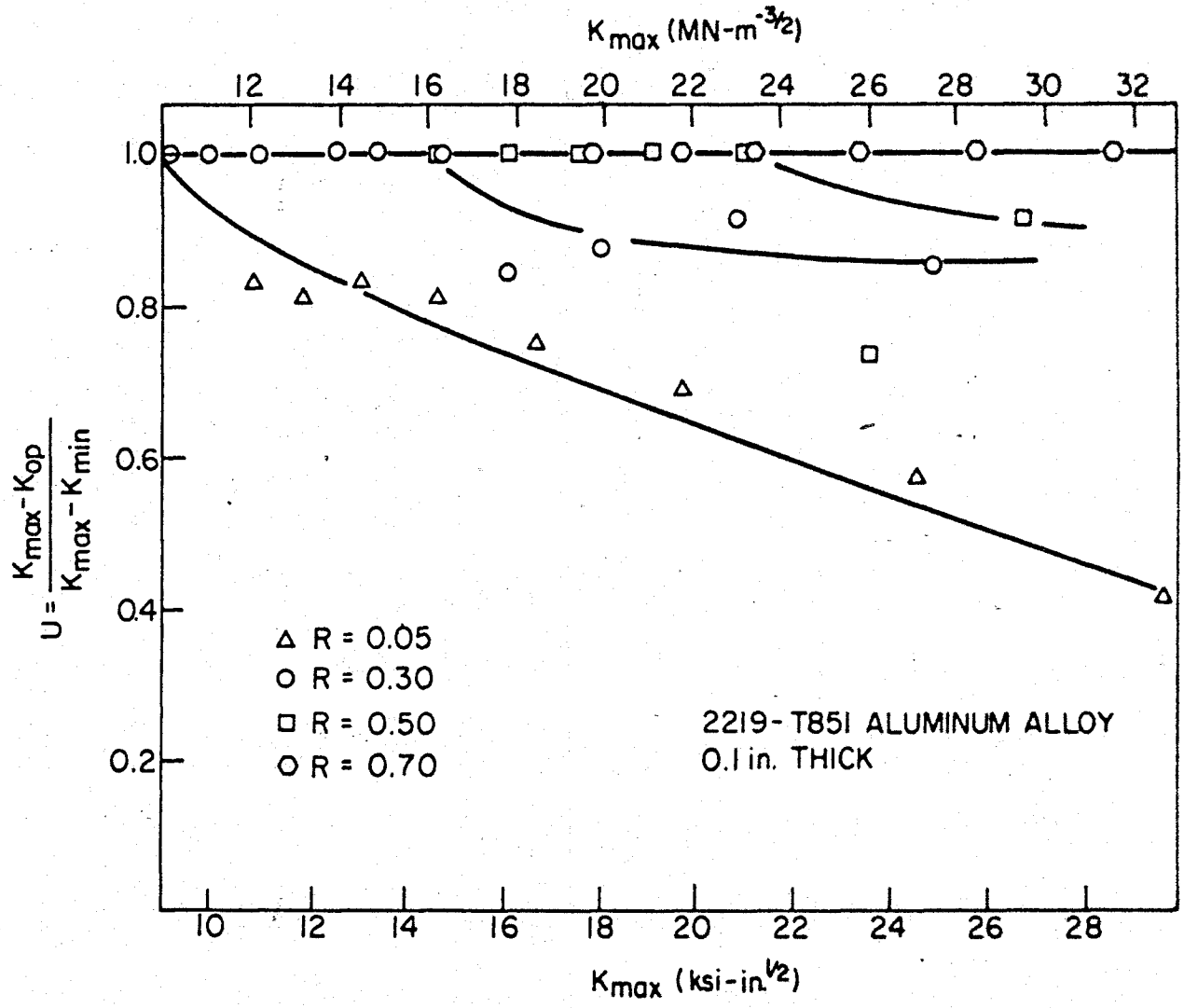

Figure 9: Relationship between U and K_{max} at different stress ratios for 0.1-in. (0.254cm)-thick specimens.

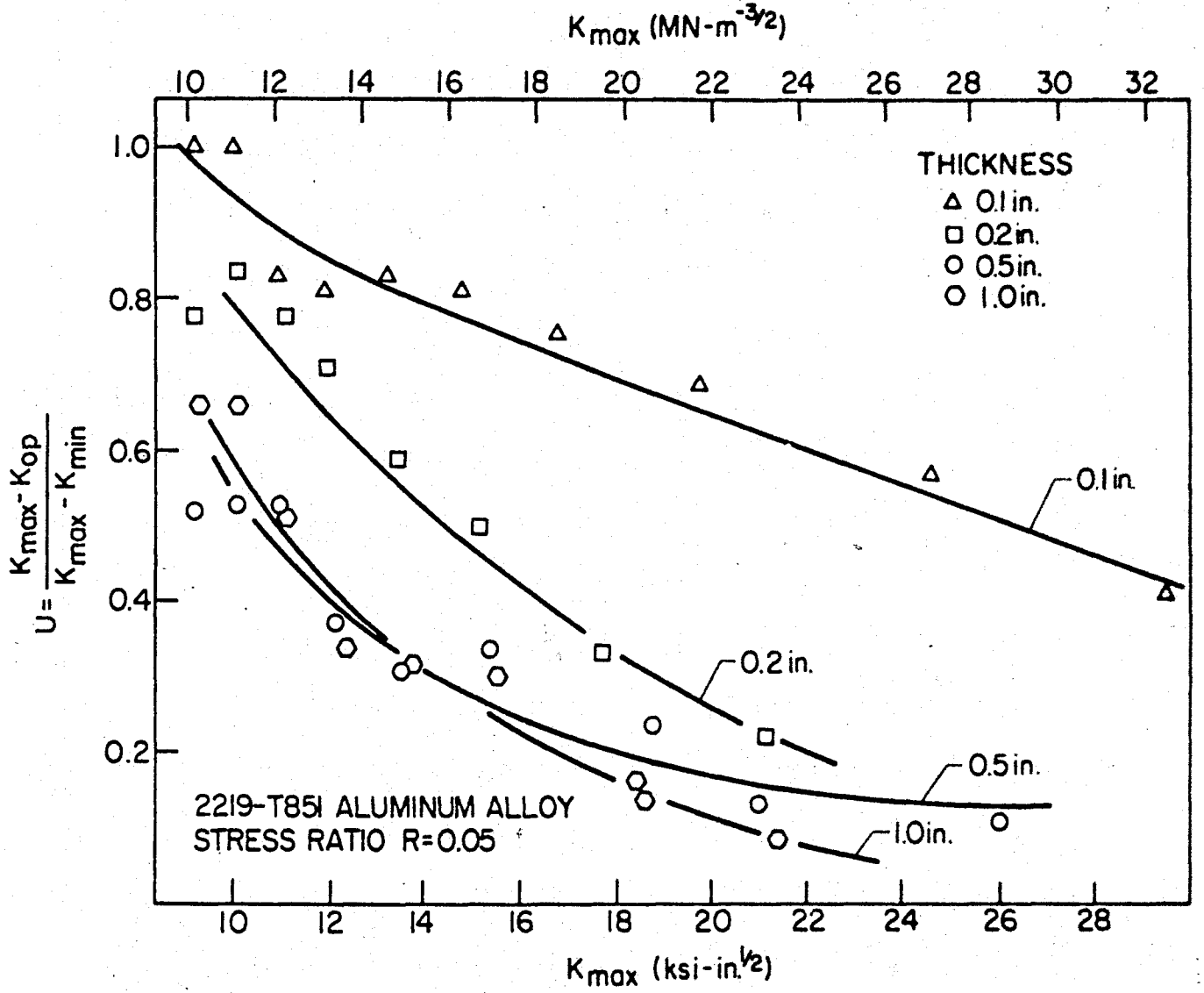

Figure 10: Relationship between U and K_{max} at R = 0.05 for different thickness specimens.

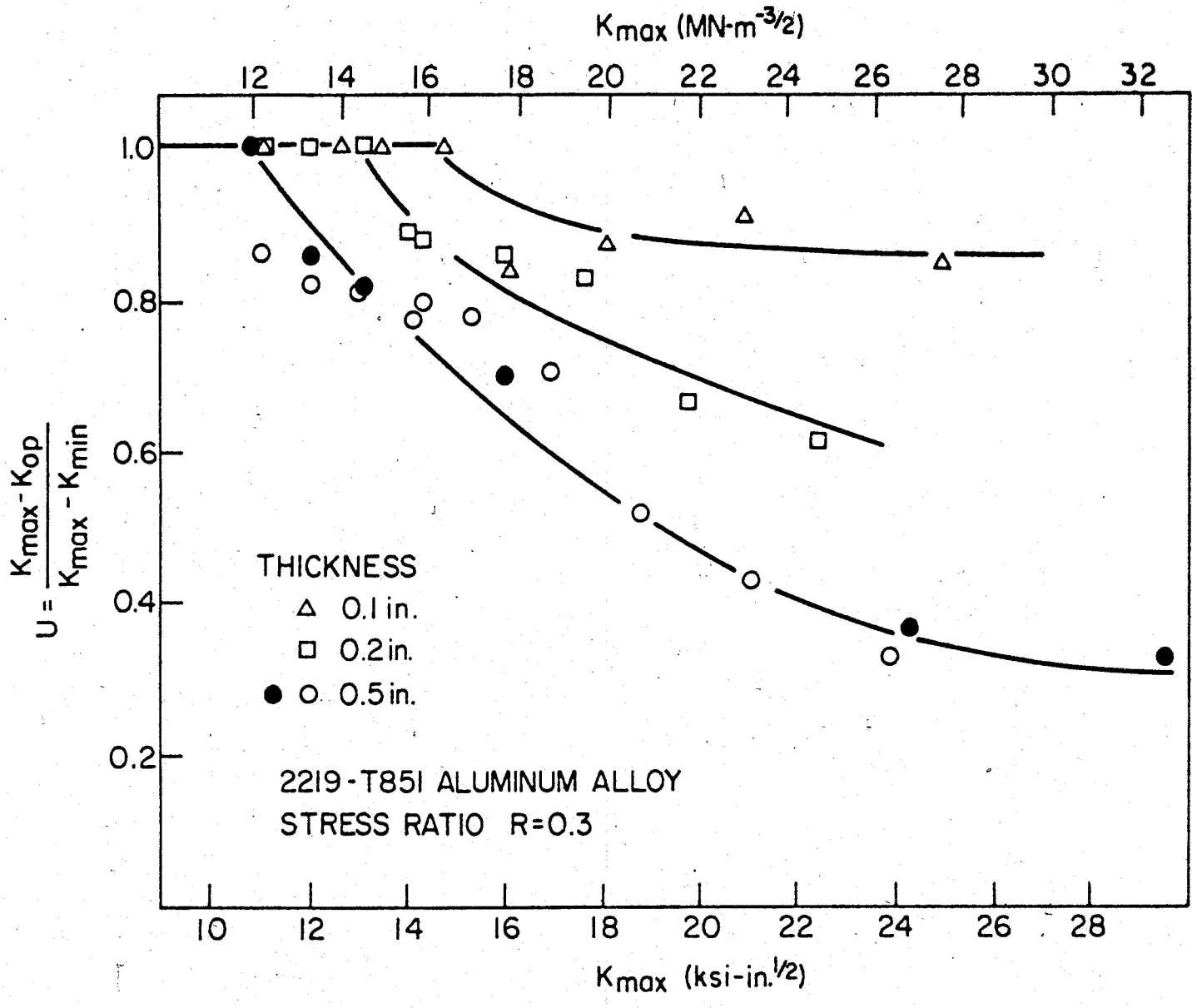

Figure 11: Relationship between U and K_{max} at R = 0.3 for different thickness specimens.

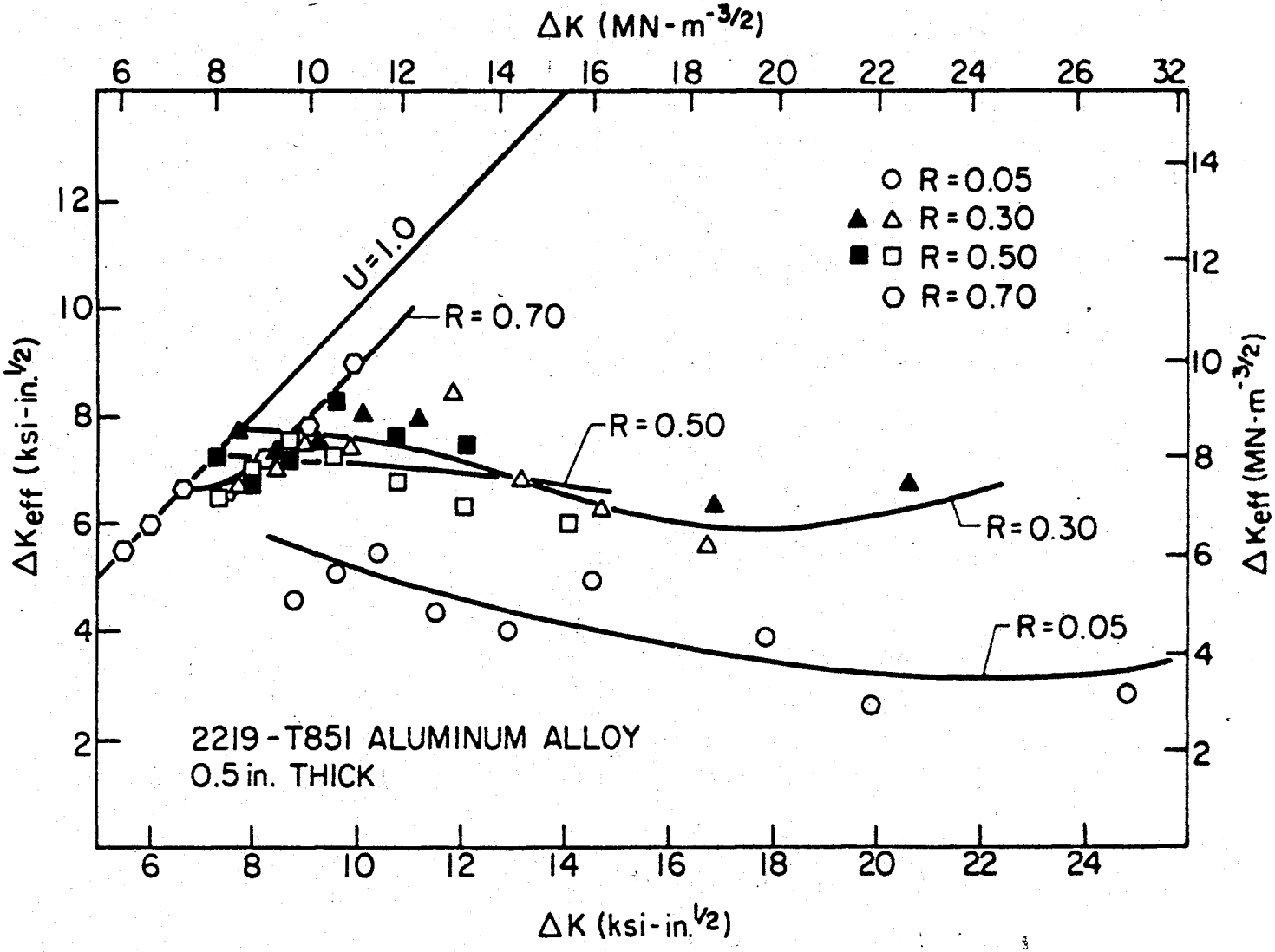

Figure 12: Relationship between ΔK_{eff} and ΔK at different stress ratios for 0.5-in. (1.27 cm)-thick specimens.

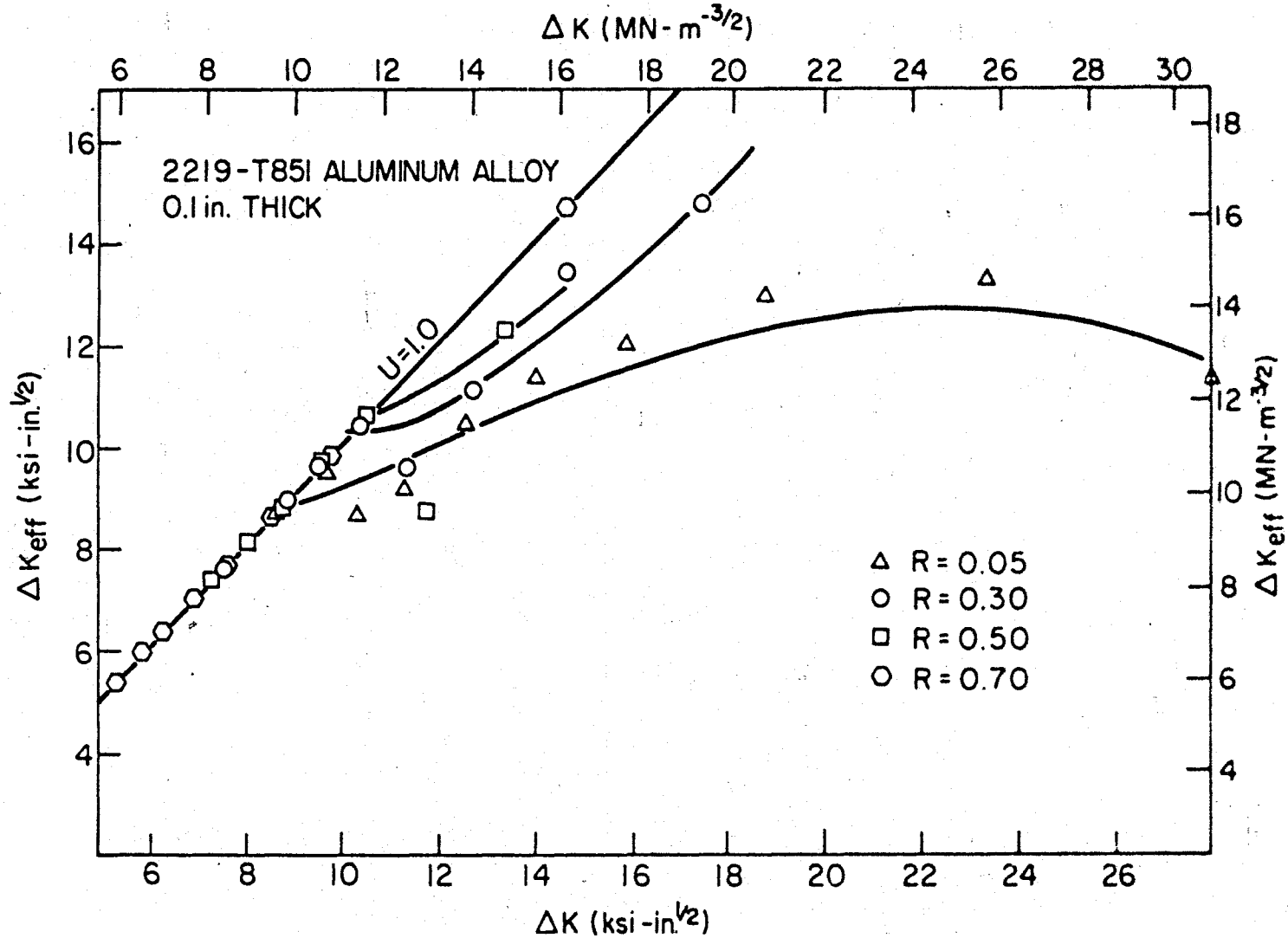

Figure 13: Relationship between ΔK_{eff} and ΔK at different stress ratios for 0.1-in. (0.254 cm)-thick specimens.

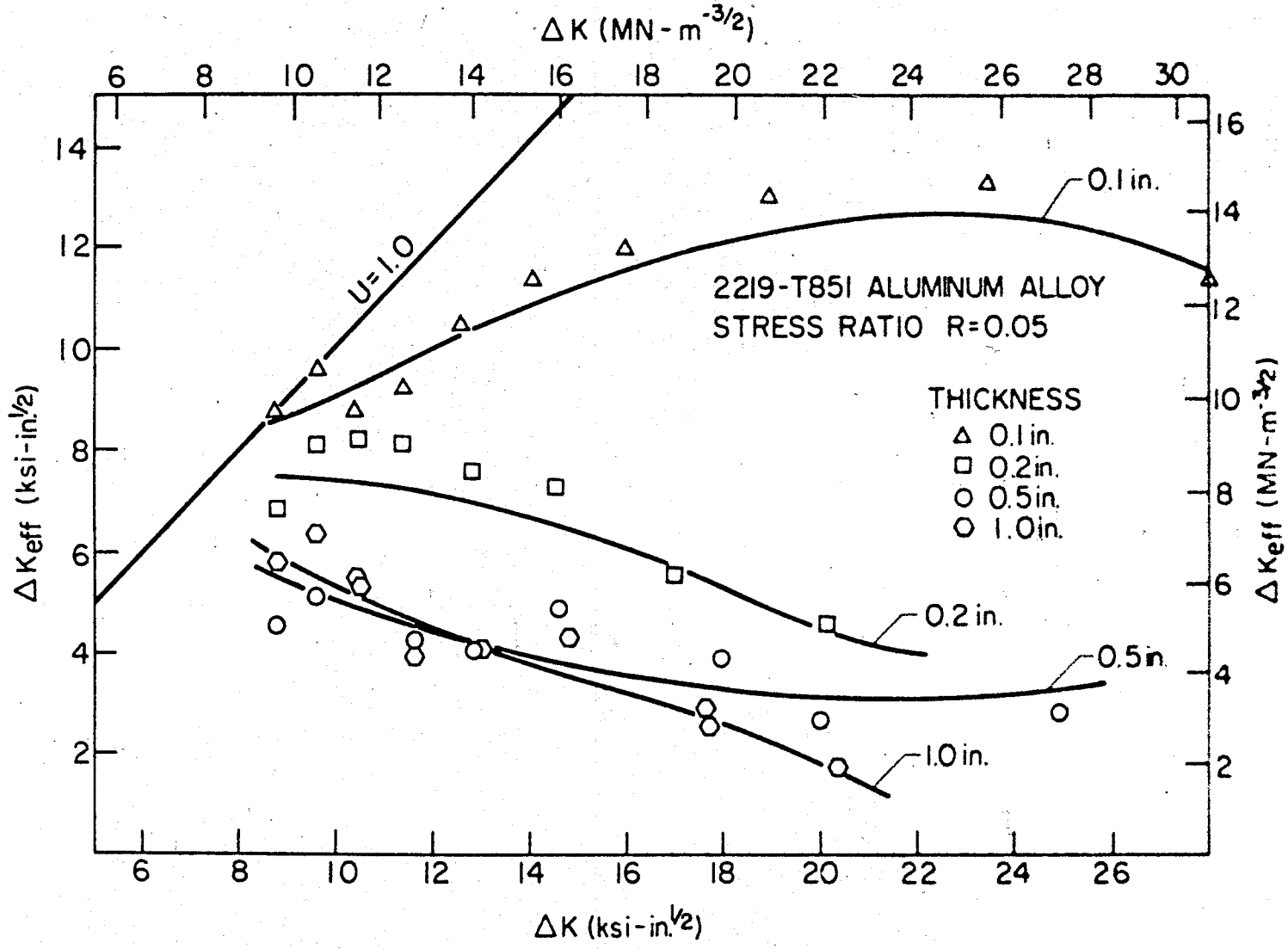

Figure 14: Relationship between ΔK_{eff} and ΔK at R = 0.05 for different thickness specimens.

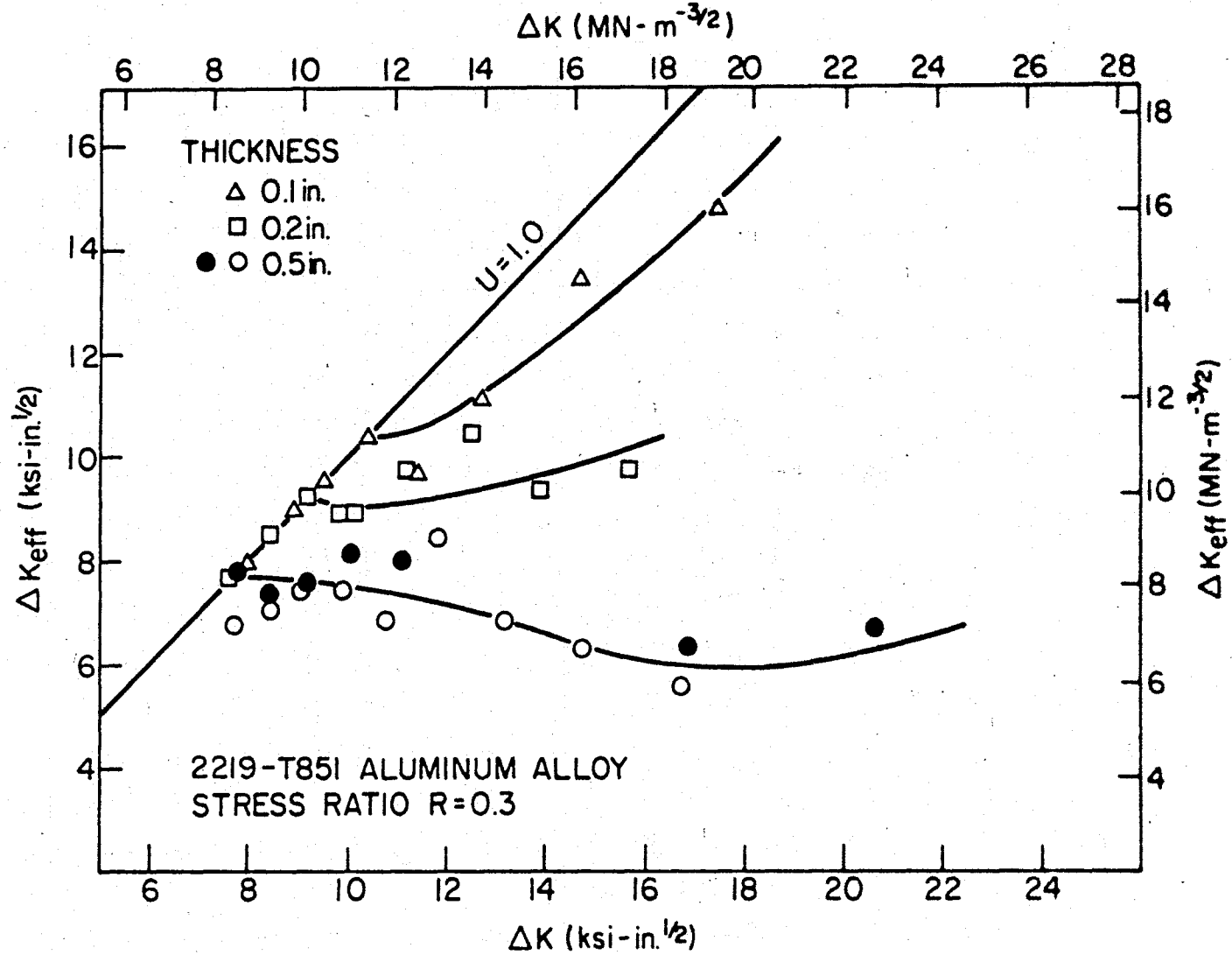

Figure 15: Relationship between ΔK_{eff} and ΔK at R = 0.3 for different thickness specimens.

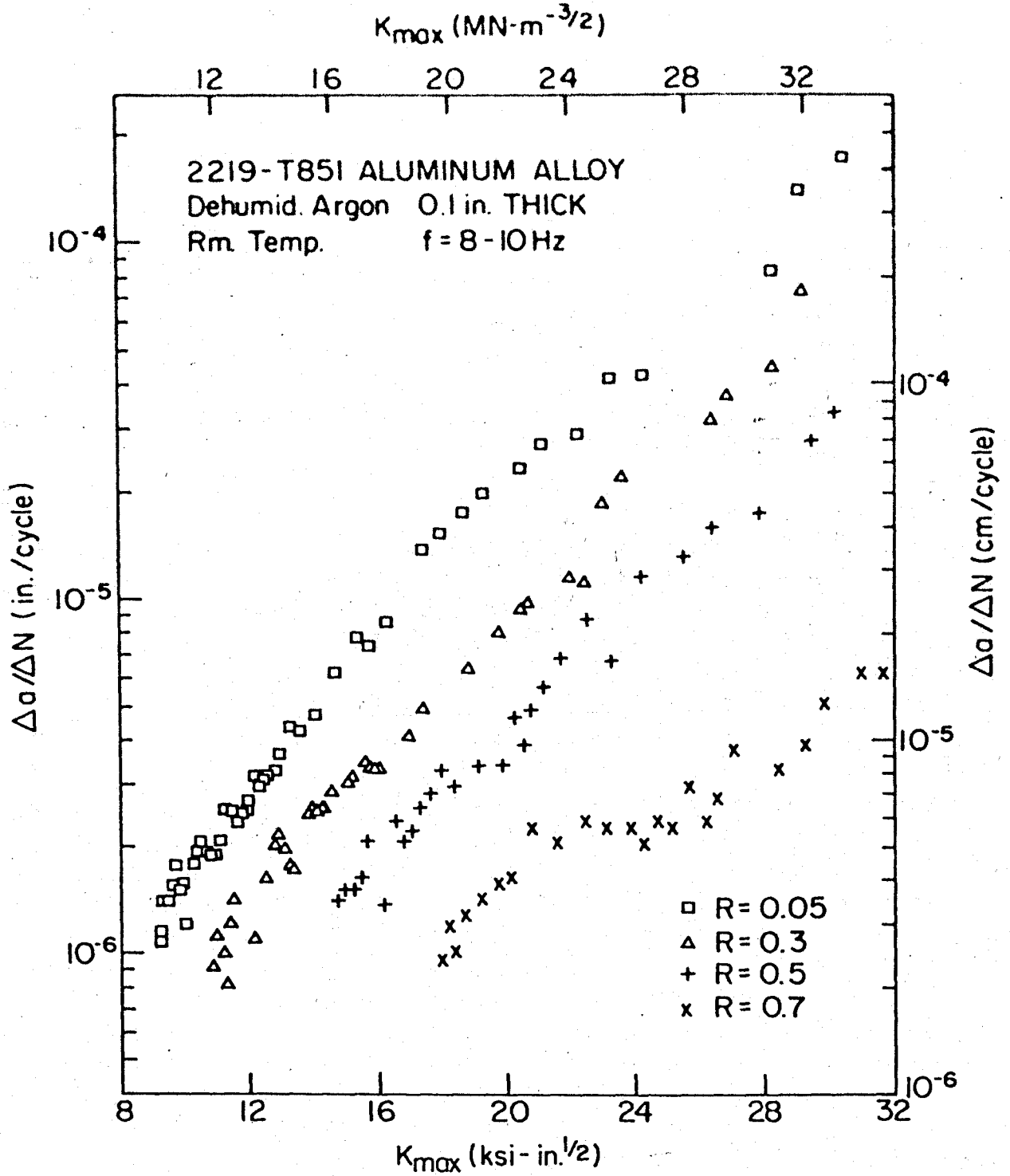

Figure 16a: Relationship between $\Delta a/\Delta N$ and K_{max} at different stress ratios for 0.1-in. (0.254 cm)-thick specimens tested in dehumidified argon at room temperature.

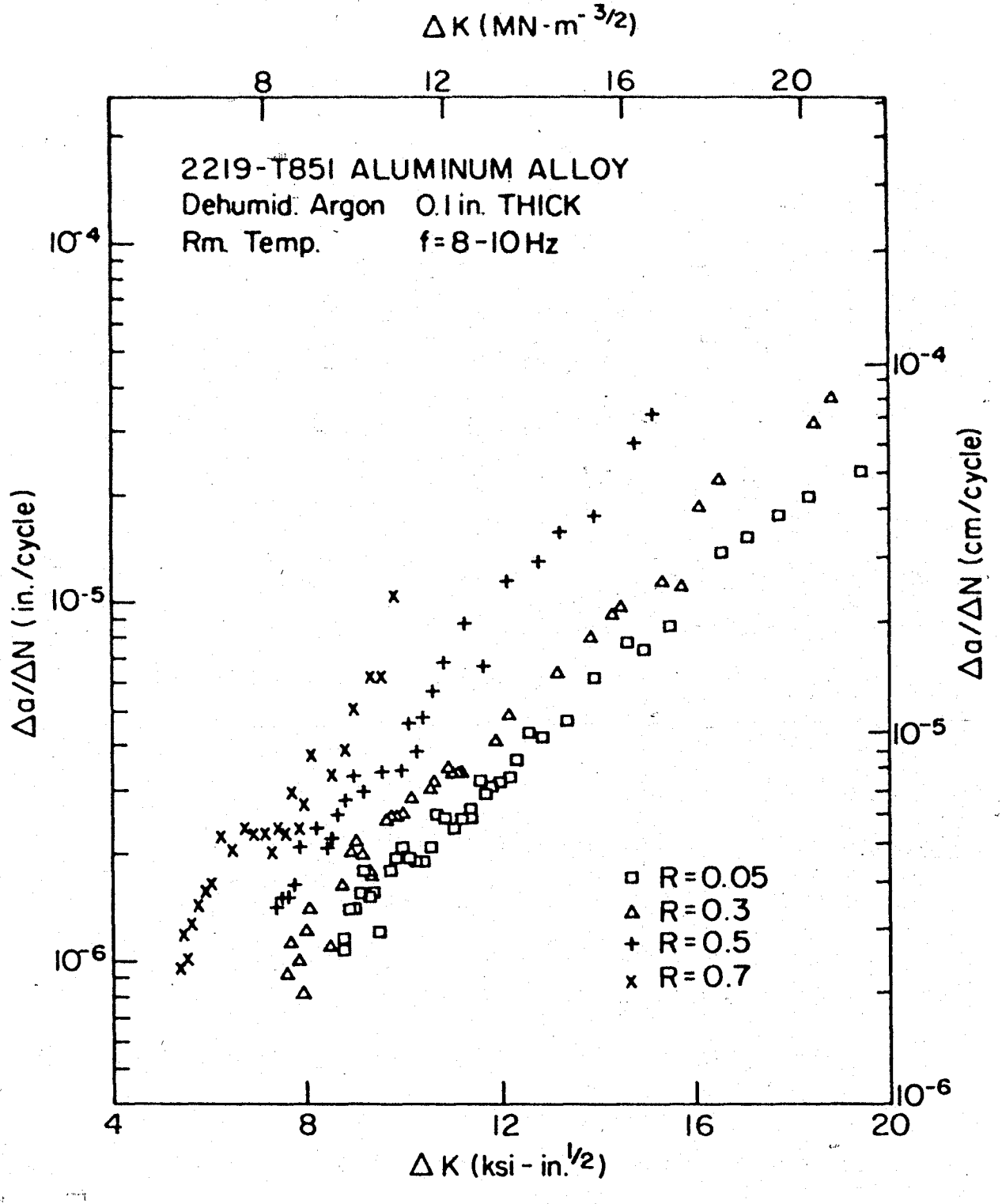

Figure 16b: Relationship between $\Delta a/\Delta N$ and ΔK at different stress ratios for 0.1-in. (0.254 cm)-thick specimens tested in dehumidified argon at room temperature.

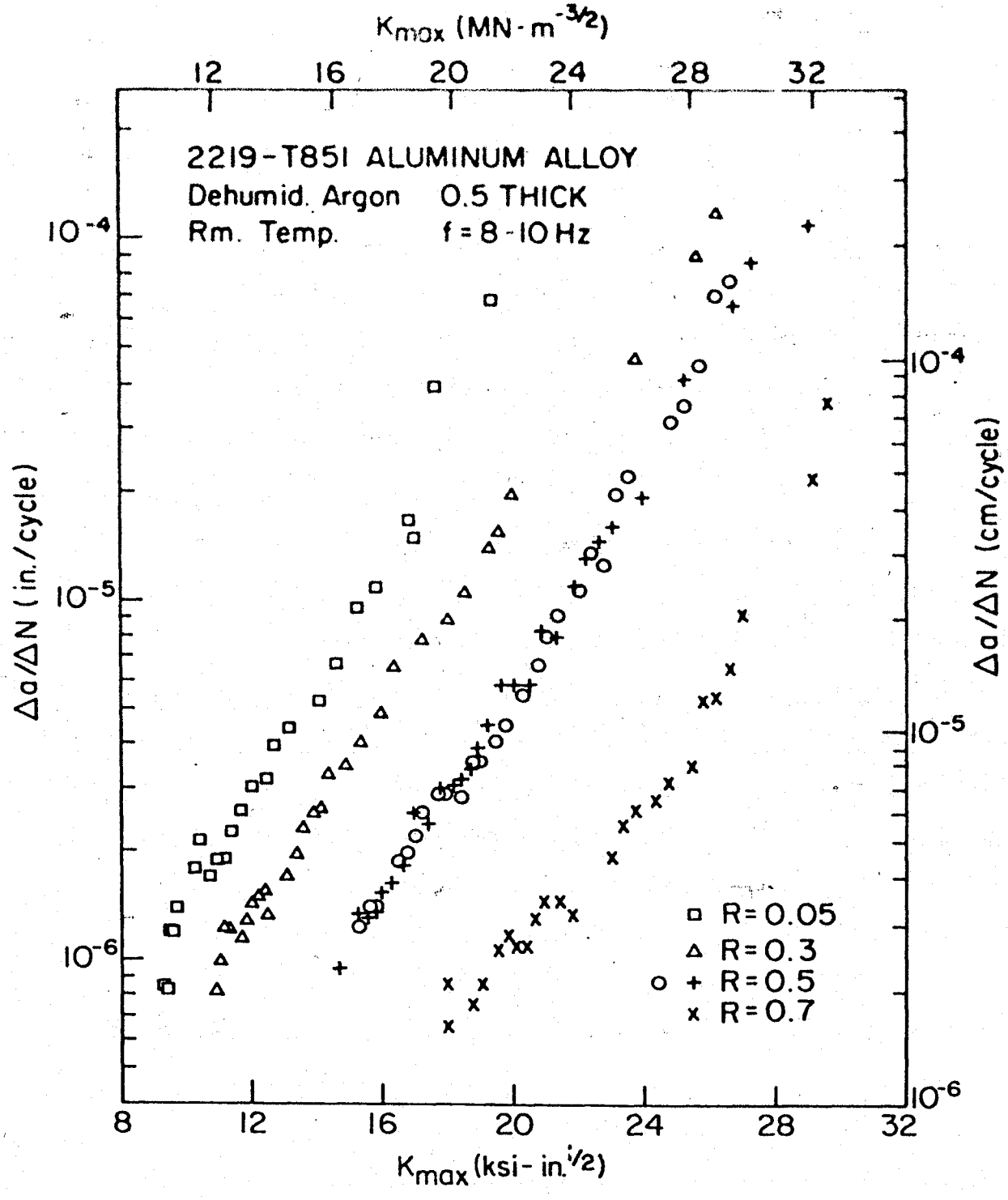

Figure 17a: Relationship between $\Delta a/\Delta N$ and K_{max} at different stress ratios for 0.5-in. (1.27 cm)-thick specimens tested in dehumidified argon at room temperature.

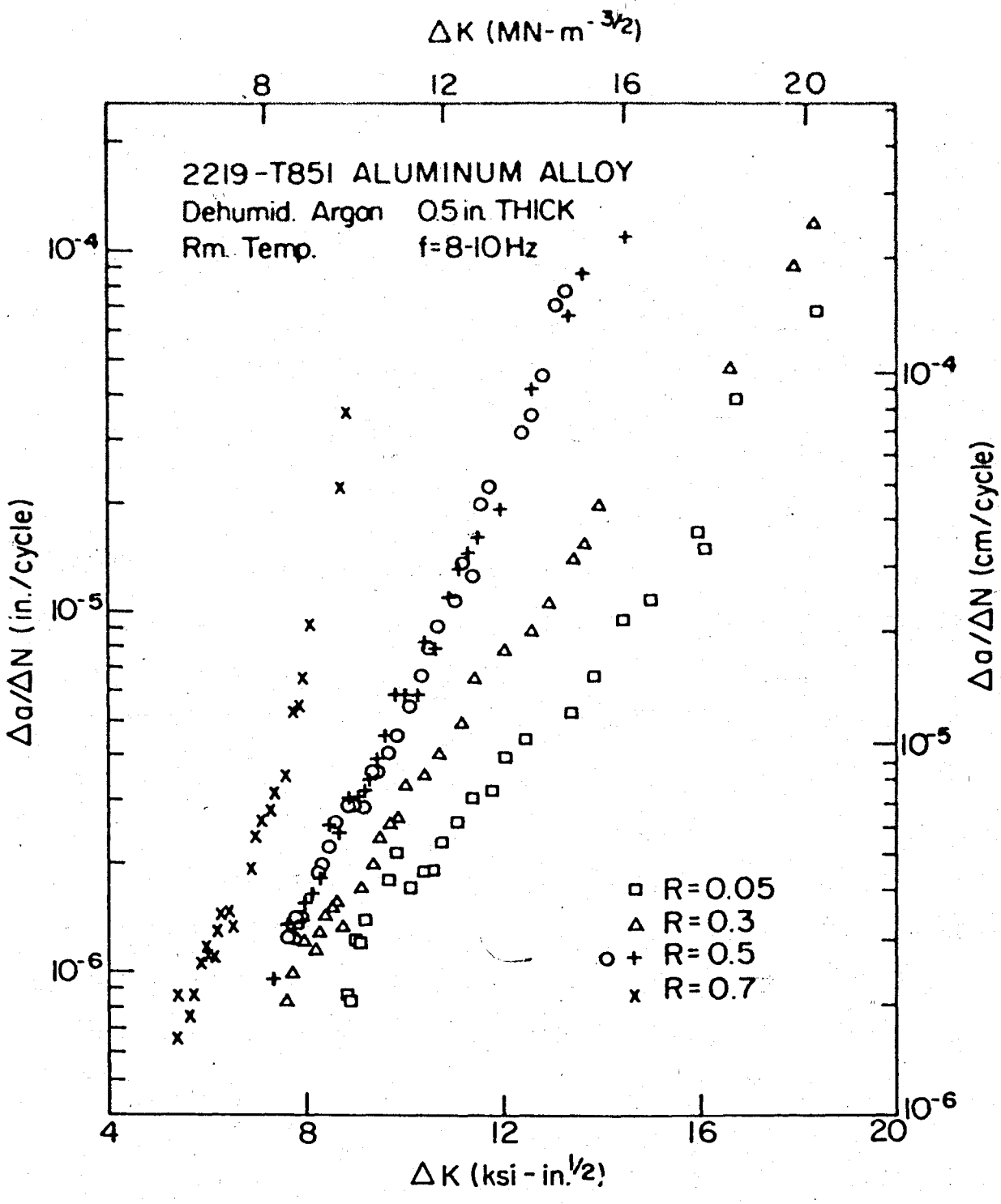

Figure 17b: Relationship between Δa/ΔN and ΔK at different stress ratios for 0.5-in.(1.27 cm)-thick specimens tested in dehumidified argon at room temperature.

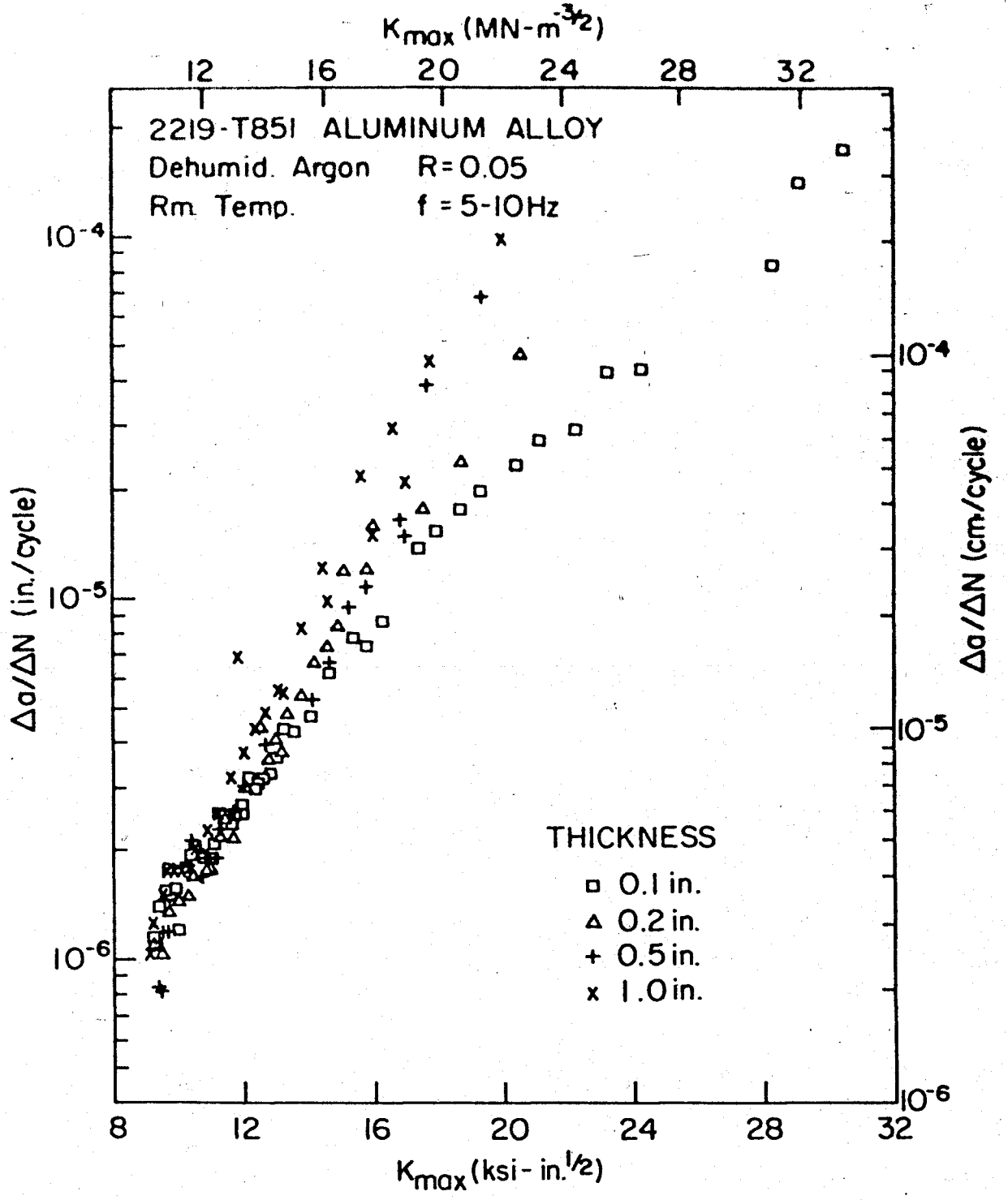

Figure 18a: Relationship between $\Delta a/\Delta N$ and K_{max} at R = 0.05 for different thickness specimens tested in dehumidified argon at room temperature.

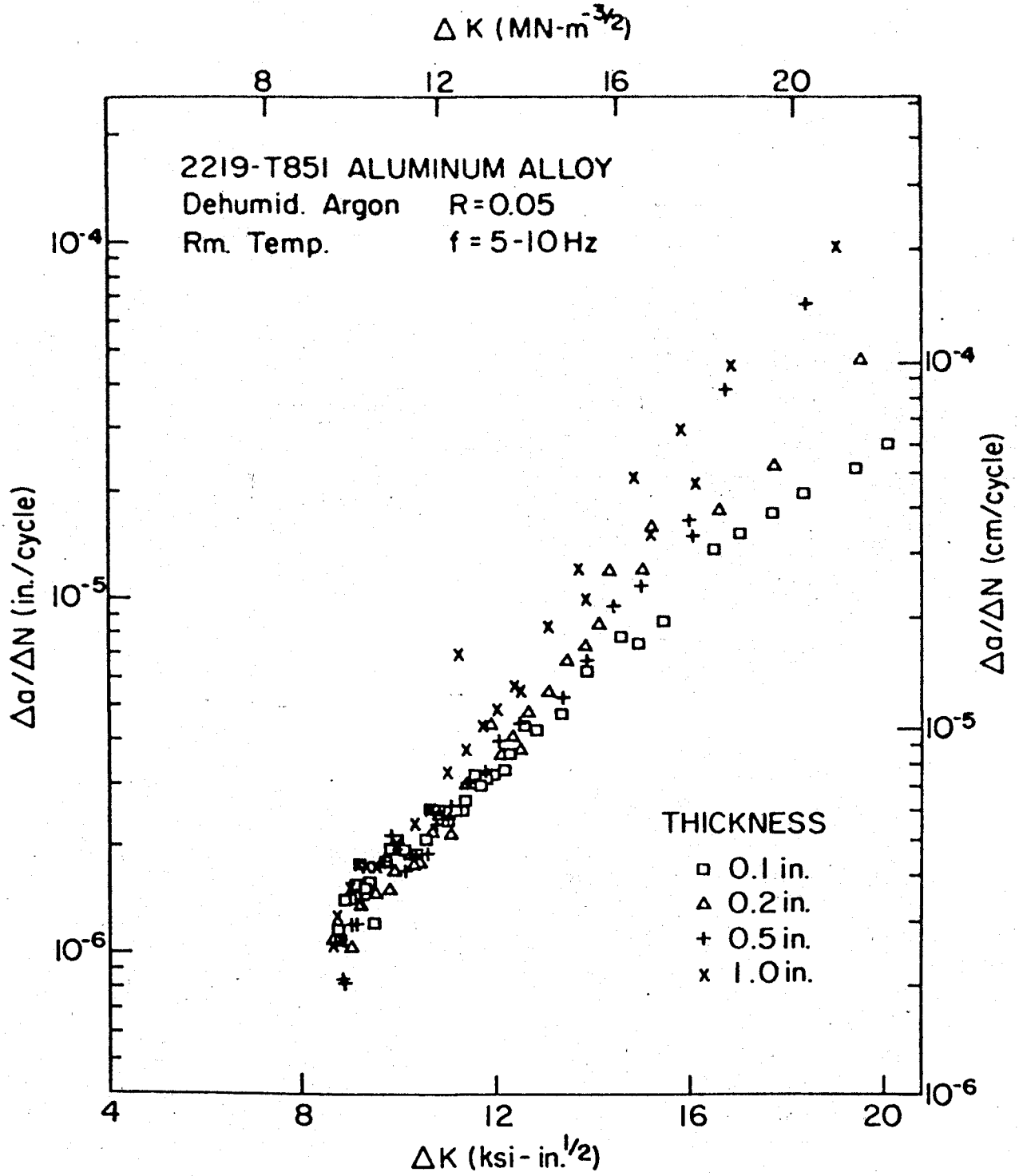

Figure 18b: Relationship between $\Delta a/\Delta N$ and ΔK at R = 0.05 for different thickness specimens tested in dehumidified argon at room temperature.

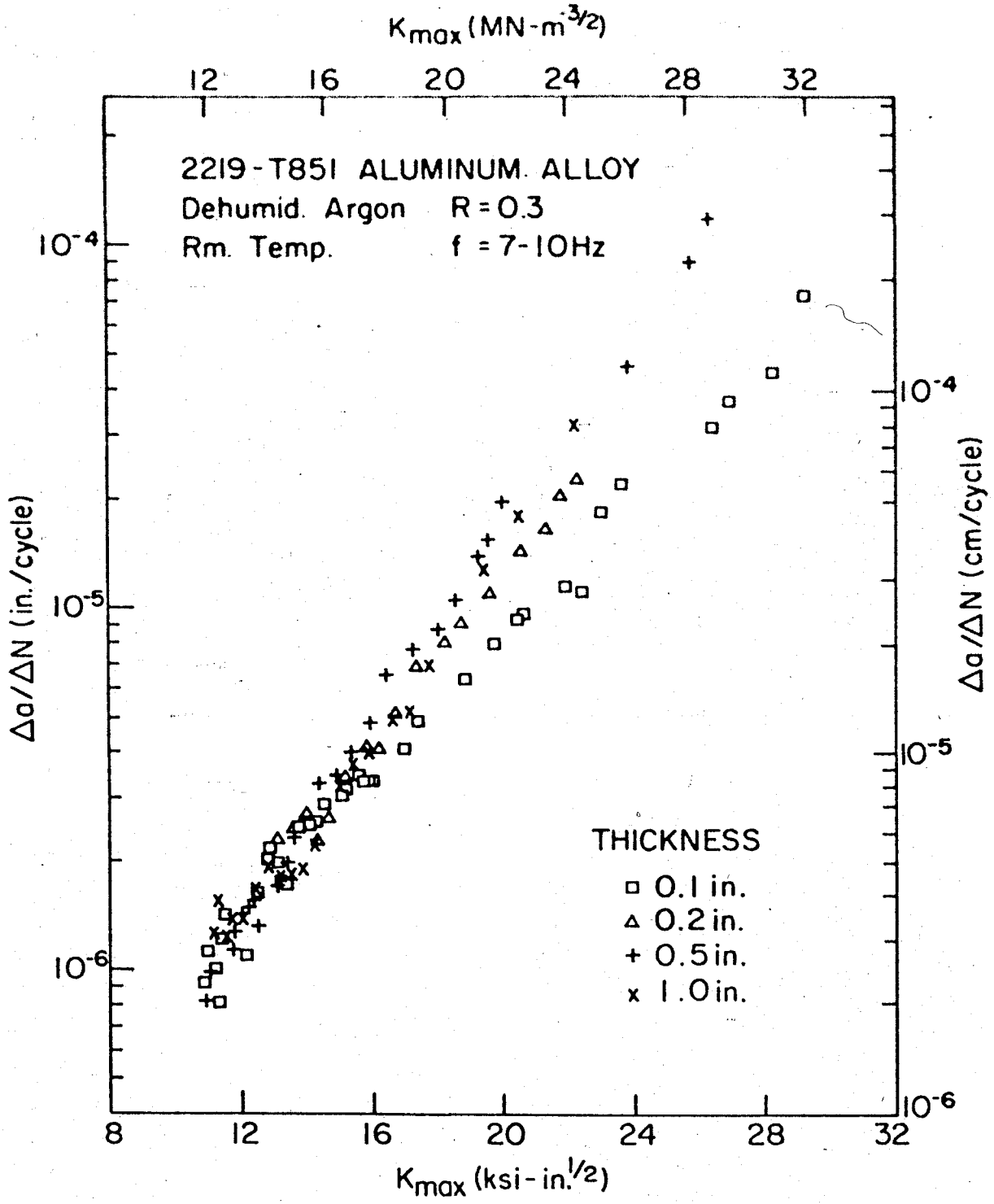

Figure 19a: Relationship between $\Delta a/\Delta N$ and K_{max} at R = 0.3 for different thickness specimens tested in dehumidified argon at room temperature.

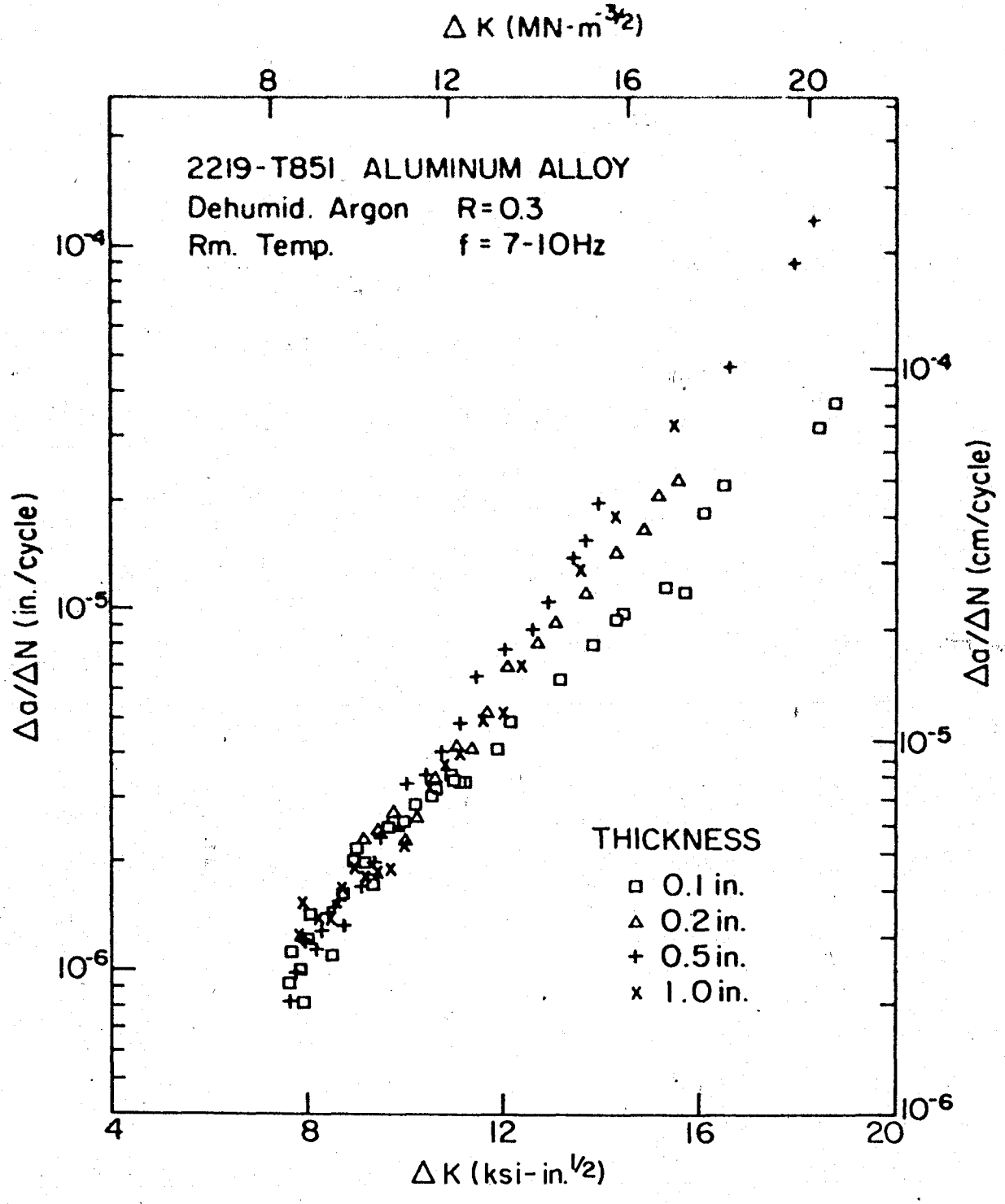

Figure 19b: Relationship between $\Delta a/\Delta N$ and ΔK at R = 0.3 for different thickness specimens tested in dehumidified argon at room temperature.

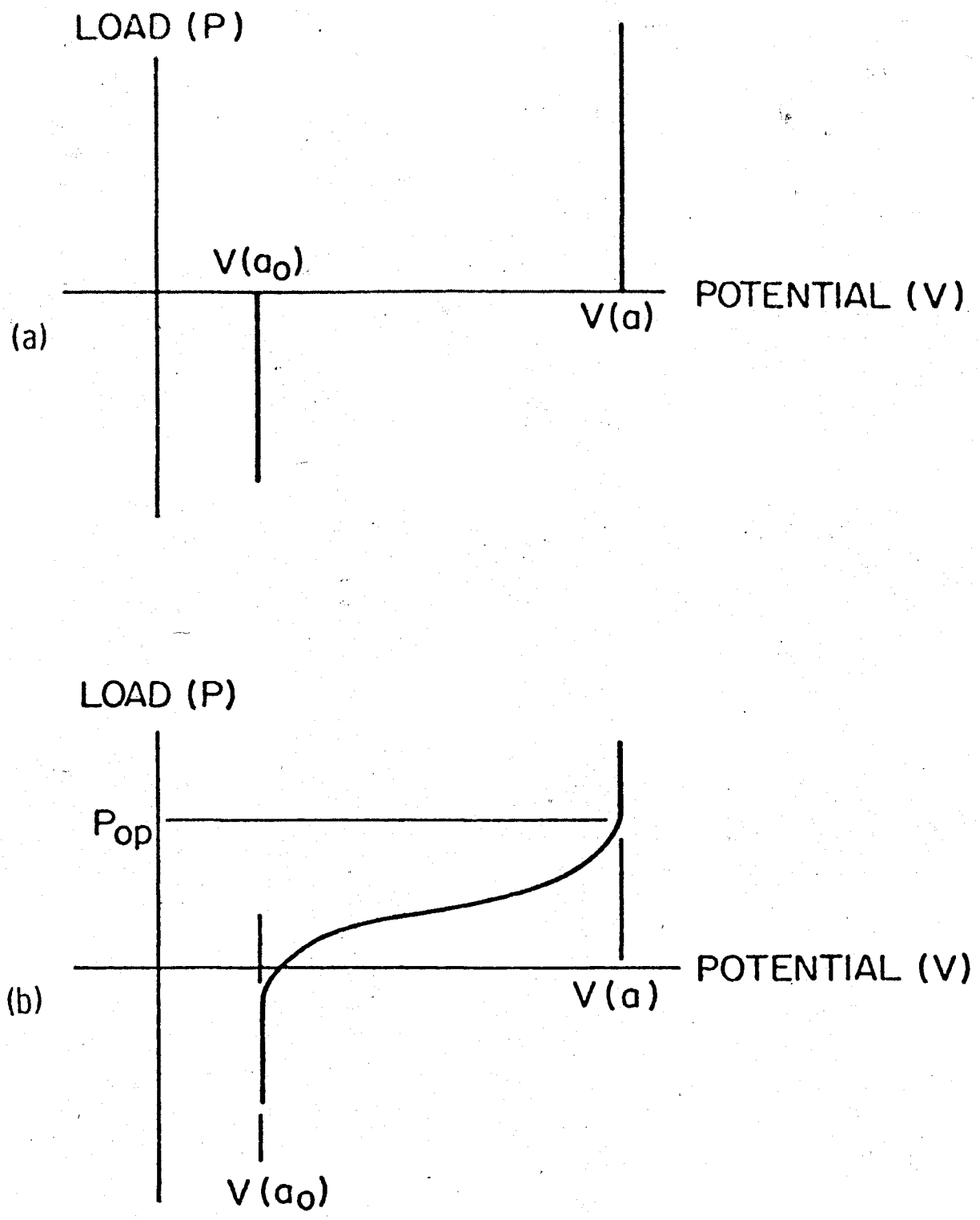

Figure 20: Schematic illustrations of load versus change in electrical potential (a) for an idealized crack in an elastic medium, and (b) for a well-behaved real crack

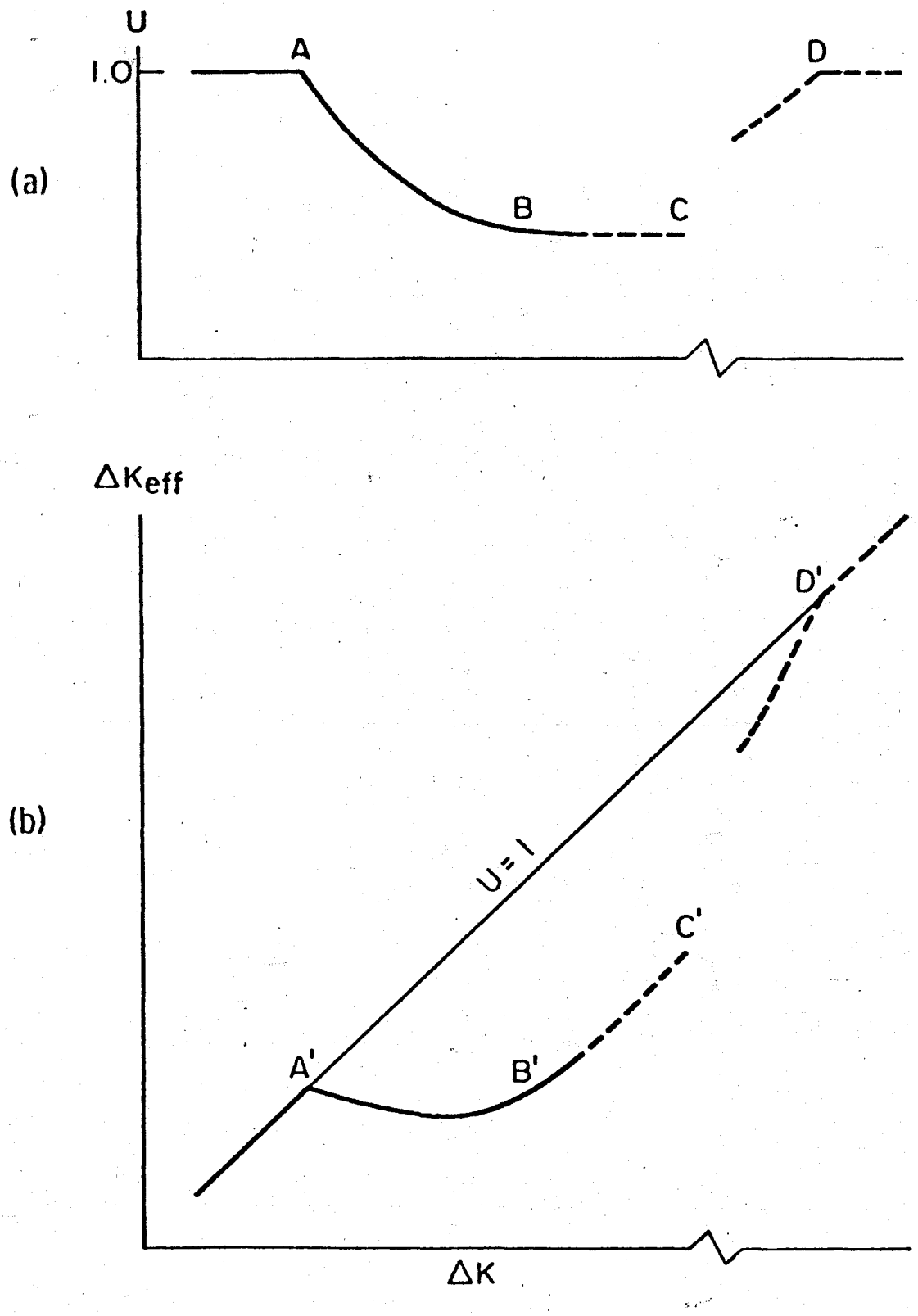

Figure 21: Schematic diagrams showing the general trend for (a) U versus K_{max}, and (b) ΔK_{eff} versus ΔK.

REFERENCES

1. H. A. Wood and W. J. Trapp, Eng. Fracture Mech. 5, p.119 (1973).

2. G. Sorkin, C. H. Pohler, and A. B. Stavovy, Eng. Fracture Mech. 5, p.307 (1973).

3. R. P. Wei, "Fracture Mechanics Approach to Fatigue Analysis in Design" ASME Paper No. 73-DE-22.

4. P. C. Paris, Fatigue - An Interdisplinary Approach, Syracuse University Press, p.107 (1965).

5. P. C. Paris, M. P. Gomez and W. E. Anderson, The Trend in Engineering, 13, p.9 (1961).

6. H. H. Johnson and P. C. Paris, Eng. Fracture Mech., 1, p.3 (1968).

7. P. C. Paris and F. Erdogan, Trans. of the ASME, Series D, 85, p.528 (1963).

8. R. G. Forman, V. E. Kearney, and R. M. Engle, Trans. of the ASME, Series D, 89, P.459 (1967).

9. H. W. Liu, Fatigue - An Interdisplinary Approach, Syracuse University Press, p.127 (1965).

10. H. P. Chu, Fracture Toughness and Slow-Stable Cracking, ASTM STP 559, p.245 (1974).

11. J. Fitzgerald and R. P. Wei, J. of Testing and Evaluation, 2, P.67 (1974).

12. O. E. Wheeler, Trans. of the ASME, Series D, 94, p.181 (1972).

13. J. Willenborg, R. Engle, and H. Wood, "A Crack Growth Retardation Model Using an Effective Stress Concept," AFFDL-TM-71-1-FBR(1971).

14. T. R. Brussat, Fracture Toughness and Slow-Stable Cracking, ASTM STP 559, p.298 (1974).

15. J. M. Barsom, Progress in Flaw Growth and Fracture Toughness Testing, ASTM STP 536, p.147 (1973).

16. J. M. Barsom, Fatigue Crack Growth Under Spectrum Loads, ASTM STP 595, P.217 (1976).

17. S. R. Swanson, F. Cicci, and W. hoppe, Fatigue Crack Propagation, ASTM STP 415, p.312 (1967).

18. S. H. Smith, Acoustical Fatigue in Aerospace Structures, Syracuse University Press, p.331 (1965).

19. J. P. Gallagher and H. D. Stalnaker, J. of Aircraft, 12, p.699 (1975).

20. W. Elber, Damage Tolerance in Aircraft Structures, ASTM STP 486, p.230 (1971).

21. E. F. J. von Euw, R. W. Hertzberg, and R. Roberts, Stress Analysis and Growth of Cracks, ASTM STP 513, p.230 (1972).

22. V. W. Trebules, Jr., R. Roberts, and R. W. Hertzberg, Progress in Flaw Growth and Fracture Toughness Testing, ASTM STP 536, p.115 (1973).

23. R. C. Rice and R. I. Stephens, Progress in Flaw Growth and Fracture Toughness Testing, ASTM STP 536, p.95 (1973).

24. O. Buck, J. D. Frandsen, and H. L. Marcus, Fatigue Crack Growth Under Spectrum Loads, ASTM STP 595, p.101 (1976).

25. O. Buck, J. D. Frandsen, and H. L. Marcus, Eng. Fracture Mech., 7, p.167 (1975).

26. R. A. Schmidt and P. C. Paris, Progress in Flaw Growth and Fracture Toughness Testing, ASTM STP 536, p.79 (1973).

27. A. Ohta and E. Sasaki, Int. J. of Fracture, 11, p.1049 (1975).

28. W. Elber, Fatigue Crack Growth Under Spectrum Loads, ASTM STP 595, p.236 (1976).

29. P. E. Irving, J. L. Robinson, and C. J. Beevers, Int. J. of Fracture, 9, p.105 (1973).

30. V. Bachmann and D. Munz, Int. J. of Fracture, 11, p.713 (1975).

31. P. E. Irving, J. L. Robinson, and C. J. Beevers, Int. J. of Fracture, 11, p.1055 (1975).

32. V. Bachmann and D. Munz, Int. J. of Fracture, 12, p.167 (1976).

33. R. Roberts and R. A. Schmit, Int. J. of Fracture Mech., 8, p.469 (1972).

34. W. N. Sharp, Jr. and A. F. Grandt, Jr., "A Laser Interferometric Technique for Crack Surface Displacement Measurements," AFML-TR-74-75, Air Force Material Laboratory, Wright-Patterson AFB, Ohio.

35. T. T. Shih and R. P. Wei, Eng. Fracture Mech., 6, p.19 (1974).

36. F. J. Pitoniak, A. F. Grandt, L. T. Montulli, and P. F. Packman, Eng. Fracture Mech., 6, p.663 (1974).

37. C. K. Clarke and G. C. Cassatt, "A Study of Fatigue Crack Closure Using Electric Potential and Compliance Techniques," NASA-CR-144932 (1976).

38. J. Schijve, Fatigue Crack Growth Under Spectrum Loads, ASTM STP 595, p.3 (1976).

39. J. Schijve and W. J. Arkema, "Crack Closure and the Environmental Effect on Fatigue Crack Growth," Report VTH-217, Delft University of Technology (1976).

40. M. Katcher and M. Kaplan, Fracture Toughness and Slow-Stable Cracking, ASTM STP 559, p.264 (1974).

41. S. J. Hudak, Jr. and R. J. Bucci, "Development of Standard Methods of Testing and Analyzing Fatigue Crack Growth Rata Data," Westinghouse Research Laboratories report under Air Force Contract F33615-75-C-5064 (1975).

42. J. Good, Material Research and Standards, 1, p.389 (1961).

43. W. K. Wilson, "Analytical Determination of Stress Intensity Factors for the Manjonie Brittle Fracture Test Specimen," Report No. WERL-0029-3, Westinghouse Research Laboratories (1965).

44. W. K. Wilson, "Optimization of WOL Brittle Fracture Test Specimen," Report No. 66-1B4-BTLFR-R1, Westinghouse Research Laboratories (1966).

45. H. H. Johson, Material Research Standards, 5, p.442 (1965).

46. C. Y. Li and R. P. Wei, Material Research Standard, 6, p.392 (1966).

47. R. P. Wei, Eng. Fracture Mech., 1, p.633 (1970).

48. R. P. Wei and D. L. Ritter, J. of Materials, ASTM 7, p.240 (1972).

49. R. P. Wei, Unpublished results on crack closure on a 2014-T4 aluminum alloy.

50. F. G. Nelson, P. E. Schilling and J. G. Kaufman, Eng. Fracture Mech. 4, p.33 (1972).

51. J. G. Kaufman, F. G. Nelson, Jr., and M. Holt, Eng. Fracture Mech. 1, p.259 (1968).

52. J. A. Feeney, J. C. McMillan, and R. P. Wei, Met. Trans. 1, p.1741 (1970).

53. G. R. Irwin, "Fracture Testing of High-Strength Sheet Materials Under Conditions Appropriate for Stress Analysis", U. S. Naval Research Lab. Report 5486 (1960).

54. R. P. Wei, Eng. Fracture Mech. 1, p.155 (1968).

55. R. W. Hertzberg, and E.F.J. von Euw, Met. Trans. 4, p.887 (1973).

56. L. A. Imig, Fatigue Crack Growth under Spectrum Loads, ASTM STP 595, p.251 (1976).

57. W. X. Alzos, A. C. Skat, Jr., and B. M. Hillberry, Fatigue Crack Growth under Spectrum Loads, ASTM STP 595, p.41 (1976).

58. J. C. Newman, Jr., Mechanics of Crack Growth, ASTM STP 590 (1975).

VITA

Kurt Daniel Unangst was born to Mr. and Mrs. Addison F. Unangst on September 21, 1953, in Sioux City, Iowa. He graduated from Brookfield High School, Brookfield, Ct. in June, 1971. The author then entered Lehigh University, Bethlehem, Pa., in September, 1971, where he graduated with Honors in June, 1975, receiving the degree of Bachelor of Science in Mechanical Engineering.